r.sim.terrain 1.0: a landscape evolution model with dynamic hydrology

Brendan Alexander Harmon[1], Helena Mitasova[2,3], Anna Petrasova[2,3], and Vaclav Petras[2,3]

[1]Robert Reich School of Landscape Architecture, Louisiana State University, Baton Rouge, Louisiana, USA
[2]Center for Geospatial Analytics, North Carolina State University, Raleigh, North Carolina, USA
[3]Department of Marine, Earth, and Atmospheric Sciences, North Carolina State University, Raleigh, North Carolina, USA

Correspondence: Brendan Harmon (baharmon@lsu.edu)

Nota bene: since we have restructured the manuscript, the references to sections, equations, figures, and tables in our responses refer to the revised paper.

1 Reviewer 1

Comment Although the difference between steady-state and dynamic flow regimes is discussed, the differences between the erosion regimes (e.g. detachment capacity limited, transport capacity limited, erosion-deposition and detachment limited) are less clear. A more thorough discussion of those regimes and their differences would allow for a clearer understanding of the results of the model compared to the typical characteristics associated with these regimes. On P16 L24 to L27, the results of SIMWE were compared to the characteristics typical of the simulated erosion regime. Establishing the characteristics of the erosion regimes earlier, perhaps after the explanation of the flow regimes, would give the reader more clarity regarding what influences these regimes and how the model compares to real-world characteristics.

Response We have restructured the paper and now thoroughly discuss soil erosion-deposition regimes in Section 2.1.2 with equations 6-9.

Comment Given that the study area has information for 2012 and 2016, one possible improvement is to compare the model results to the observed difference between those two years. Although the results section on P16 compares the modelled characteristics with typical erosion regime characteristics, the comparison to the 2012-2016 data is limited to P16 L23. Adding validation of model results against observed landscape evolution would show the strengths of the model.

Response This is a model description paper, rather than a model evaluation paper. While we have added a quantitative comparison of volumetric change to the paper, we plan to conduct a rigorous quantitative evaluation of r.sim.terrain in future work. Because the models are for different erosion regimes, different study sites each with a different dominant regime would be needed to quantitatively assess each model against a relevant baseline. A more accurate, higher frequency of high resolution topographic surveying is also needed, ie. monthly surveys with terrestrial lidar or unmanned aerial systems. We have added plans for future work to the new Discussion section.

Comment Another possible improvement is to more clearly present the limitations of the model in their own section. On P4 L22, the model limitation of not modelling fluvial processes is mentioned. By having a clear limitations section with information about model assumptions, the reader is more informed about the model and how it may affect results.

Response We have added a paragraph on the limitations of the model to a new Discussion section.

Comment The quality of the figures and the presentation of spatial data is a major issue of the paper. With the exception of Figure 1, many of the figures are too small to be analysed in detail. The legends are pixelated (Figure 4c, 4e, and 4f) or cut off (Figure 5a and 5d). The legends for the landform maps (Figures 5b, 5e, 6b, and 6e) would benefit from the labels presented in Figures 4e and 4f. The colours chosen for the figures could also be improved. For example, Figure 2b shows a landscape with yellow/orange/blue colours but the colour bar only shows a scale of yellow to orange. Using the hillshade layer seems to darken the colours within the gully and the reader is unable to clearly see those colours. The use of a 3D top-down view in Figure 5 makes it difficult to see what is occurring within the gully area where the differences are most important. Some figures are presenting differences (Figure 5c, 5f, 6c) that cannot be visualised clearly because most of them are occurring within the gully area and thus “blocked” by the 3D view and hillshade. Overall, the figures can be improved, especially for visualisation of the key results and differences, and that would contribute to the overall quality of the paper. The differences may be better visualised through 2D top-down view, or 2D cross-sections, or even zooming into the most critical areas of the gully. At the watershed scale and using the current visualisation, the results are difficult to visually interpret and do not supplement the written results well.

Response All figures have been redone. They have newer higher resolution legends, scale bars, and north arrows. Figures 3 and 6-9 include details zoomed in on a drainage area (Drainage Area 1) within the subwatershed. These figures are now focused on the main channel of the gully and should show more legible detail. Figure 4b shows the drainage areas. In addition to zooming in on Drainage Area 1, Figures 6-9 are now presented in 2x2 columns and rows, rather than 2x3 columns and rows so that the images are larger and more detail is visible. Selected figures are now 2D rather than 3D maps. We have changed or removed hill shading from select maps to improve their legibility.

Comment P3, L22: According to Dabney et al. (2014), RUSLER refers to RUSLE2-Raster which is a distributed form of the Revised Universal Soil Loss Equation Version 2, which is normally referred to as RUSLE2. The paper is referring to the Revised Universal Soil Loss Equation Version 2 when it is using the RUSLE2-Raster acronym. Please clarify if the paper is referring to RUSLER or RUSLE2.

Response We have replaced this with: “Gully erosion has been simulated with RUSLE2-Raster (RUSLER) in conjunction with the Ephemeral Gully Erosion Estimator (EphGEE) (Dabney et al., 2014).”

Comment P6, L11 to P7, L6: This paragraph would be better presented in a table or a flowchart showing how the model switches erosion regimes based on rainfall intensity.

Response To more clearly present how soil erosion regimes are handled in this model we have added Section 2.1.2 Erosion-Deposition Regimes. We have also removed the detachment limited and transport limited cases for SIMWE to avoid unnecessary complexity in the paper and results.

Comment P14, L11 to L13: Additional detail about how the information about K-factor, C-factors, Manning’s, and runoff rates were derived would be useful for those who wish to apply the model in their study area.

Response We have added links to detailed instructions for deriving these maps in the tutorial. We have also added a link to our data log with a complete record of the commands used to process the sample data.

Comment P3, L17: Since LIDAR is an acronym for Light Detection and Ranging, mentions of LIDAR should be in capitals and the first instance should have the accompanying meaning of LIDAR.

Response We have followed the recommendation in the paper “Let’s agree on the casing of lidar” (Deering & Stoker, 2014), which shows that 65% of literature uses lidar (including USGS), while 17% use LIDAR and 14% use LiDAR. Their reasoning is that lidar is the most common usage, the original usage, and the usage recommended by style manuals However, the latest issues of ISPRS journals use LiDAR, so we will defer to the journal editor on what their standard should be. For our part we prefer to follow USGS usage of lidar.

Deering, Carol & Stoker, Jason. (2014). Let’s agree on the casing of lidar. Lidar Magazine. 4. 48-51. http://lidarmag.com/wp-content/uploads/PDF/LiDARNewsMagazine_DeeringStoker-CasingOfLiDAR_Vol4No6.pdf

Comment P4, L28 and similar headings: For these headings, referee suggests formatting as follows “Simulation of Water Erosion Model (SIMWE)” and only using the acronym on the following line.

Response Reformatted as recommended.

Comment P6, Table 1: Citation of “(Dennis C. Flanagan et al., 2013)” should just be “(Flanagan et al., 2013)”.

Response Citation fixed as recommended.

Comment P10, L15: The addition of "(a)" after "The upslope contributing area per unit width" would allow for a clearer connection to Equation 12.

Response Variable added as recommended.

Comment P13, L14 and P14, L1: Scientific names should be italicised.

Response Scientific names have been italicized.

2 Reviewer 2

Comment The text has detailed descriptions of the underlying theory behind many components of the overall simulation model (section 2) but does not indicate how these relate to one another. While there are many colorful figures of landscape evolution results, there is no representation of the model itself (e.g., UML or other flow-chart-like visualization) – nor is there much in the way of narrative description of how the model actually works to combine the described elements.

Response We have added a conceptual diagram of the model as Figure 2.

Comment Section 3.2 describes several experimental runs with the simulation model. These experiments are summarized in Table 3. However, we have no quantitative information about the results of the experiments. There is no information about whether each experiment was run only once or repeated–or whether repetition is needed or not because each parameter setting produces or does not produce only one outcome. Although the simulation is situated in a realistic setting based on digital data from Ft. Bragg, NC, the rationale for some of the parameterizations are not given, particularly the important rainfall settings. These might be completely reasonable, but the authors should indicate if these are based on empirical rainfall data or have another basis (e.g., extreme values to test the model sensitivity).

Response Repeat runs are not needed because RUSLE and USPED are empirical, non-stochastic models and produce only one outcome. SIMWE path sampling method includes stochastic component for solving the continuity equations but this relates to the accuracy of the solution, e.g., a high number of walkers reduces the numerical error associated with the path sampling solution. We have added a discussion of this to the paragraph on limitations. We have added more information about the parameters of the simulations in subsections 3.1 and 3.2 on the study site and simulations. This includes a link to detailed instructions for the sample data and a discussion of the design storms and their rationale.

Comment The authors have collected detailed, time series, LiDAR and orthophoto data from the test area represented in the simulation. But they make no attempt to compare the simulation experiments with these data in any quantitative sense. Rather they give only brief, subjective assessments of model behavior. It would seem rather easy to compare the model with the empirical data to see which experiments are better or worse fits and in what ways.

Response We consider this manuscript a model description paper, rather than a model evaluation paper. While we have added a quantitative comparison of volumetric change to the paper, we plan to conduct a rigorous quantitative evaluation of r.sim.terrain in future work. Because the models are for different erosion regimes, different study sites with a different dominant regimes may be needed to quantitatively assess each model against a relevant baseline. A higher frequency of high resolution topographic surveying would also help, ie. monthly surveys with terrestrial lidar or unmanned aerial systems. We have added plans for future work to the conclusion.

Comment Finally, I downloaded and installed r.sim.terrain into GRASS and tried to run it. I strongly commend the authors for making the model code and test data available. This is critically important for research based on modeling like this paper. I installed r.sim.terrain into the most current version of GRASS according to the directions in the manuscript (i.e., using g.extension). Unfortunately I ran into several problems that made testing the the model impossible. First, there is a link to the test dataset in the model online help, but this link does not work. Using information in the paper, I was able to go to the GitHub site and poke around until I found the test data set and installed it into my GRASS data directory. I then followed the steps in the tutorial to simply see how it ran–thinking to compare the different overland flow and erosion/deposition methods, and time series vs. event. The command given to test the model failed initially because it was missing the rather critical “elevation” argument. So I added that. Then it started but rapidly bombed with errors related to the time series part. I copy these below. So I never did get it to run.

Response We have updated the documentation both on the manual page and the GitHub repository with the tutorial. The reviewer’s run of the model failed due to incomplete documentation rather than bugs. The input elevation raster must be in the current mapset (for registration in the temporal database), so it should be copied from the PERMANENT mapset to the current working mapset before the model is run. We have added a section with basic instructions to the manual page (https://grass.osgeo.org/grass76/manuals/addons/r.sim.terrain.html) and to the repository readme (https://github.com/baharmon/landscape_evolution). We have also written a longer tutorial (https://github.com/baharmon/landscape_evolution/blob/master/tutorial.md) that details running each model with instructions and examples for RUSLE3D, USPED, and SIMWE.

Comment However, the authors need to do a better job of explaining how the model works and not just the conceptual components included in the model. They also need to provide more information about the four experiments performed and their parameter settings. They need to provide some quantitative evaluation of the model results, including comparison with the empirical data they have collected. Finally, they need to fix some probably minor but annoying bugs in the code available for evaluation.

Response We have added a conceptual diagram of the model (Figure 2) and rewritten and expanded subsection 3.2 on the simulations and their parameters. We have added quantitative evaluation and comparison of the models and explained its limitations. We, however, would like to reiterate that this is a model description rather than evaluation paper. Finally, while there were no bugs in the code, we have fixed and expanded the documentation, which was incomplete.

3 Reviewer 3

Comment 1/title - This is a total quibble, and please feel free to ignore it, but my first reaction to ‘dynamic landscape evolution model’ was to ask (rhetorically) ‘is there any other kind’? Consider ‘landscape evolution model with dynamic hydrology’ as an alternative (admittedly a less pithy one).

Response Titled changed to “r.sim.terrain: a landscape evolution model with dynamic hydrology” as recommended.

Comment 1/5 ‘steady state or dynamic model’ could be read as implying that the entire model is steady state, not just the surface water flow rates. Suggest re-wording: ‘using either a steady state or dynamic representation of overland flow ...’

Response Reworded as recommended.

Comment 2/2 I agree with the sentiment, but suggest rewording to ‘a landscape evolution model that includes time-evolving surface water discharge’, to avoid confusion over which aspect of the model is dynamic.

Response Replaced with “A landscape evolution model with dynamic water and sediment flow. . . ”

Comment 3/8 The phrase ‘until water flow reaches steady state’ suggests that the positive feedback (presumably between deepening/widening and attraction of more surface water flow) stops at this point. I don’t think that is necessarily true; you could have a feedback between morphology and flow under steady runoff too.

Response An excellent point. Revised simply by cutting “until water flow reaches steady state.”

Response 3/11 Please explain what is meant by erosion-deposition regime.

Comment We have added a new Section 2.1.2 describing erosion-deposition regimes. This includes equations 7-11.

Response 3/14 Detachment vs transport capacity: this sounds backwards…

Comment Detachment capacity and transport capacity are now more clearly explained in Section 2.1.2 Erosion-Deposition Regimes.

Response 3/18-19 There are plenty of other papers that could be cited here, in which one or more of the listed methods was used to study gully erosion. (For example, here's a review paper that cites some TLS applications to gully erosion:
Telling, J., Lyda, A., Hartzell, P., & Glennie, C. (2017). Review of Earth science research using terrestrial laser scanning. Earth-Science Reviews, 169, 35-68.)

Response This paragraph was just meant to be a brief overview of methods, not a comprehensive review, but we have added many more references to the introduction.

Comment Figure 2: please give location in caption. Also, numbers on color bars and scale bar are barely legible.

Response We added the location to the caption and have redone the legends and scale bars at higher resolution.

Comment 6/2 typo.

Response The typo has been fixed.

Comment 6/2 I guess 'partial derivatives of the topography' means a numerical approximation of the derivative of the elevation field with respect to the two cardinal grid directions. Recommend more precision in wording here.

Response We have more clearly phrased this, explained briefly how it is computed, and added a reference to the chapter Geomorphometry in GRASS GIS (Hofierka et al., 2009) that explains the math and implementation.

Comment 6/9 'steady state dynamics' - I think I understand what you mean here, but the phrase itself is awkward (it is self-contradictory).

Response Replaced with: "r.sim.terrain simulates unsteady-state flow regimes when the landscape evolution time step is less than the travel time for a drop of water or a particle of sediment to cross the landscape, e.g. when the time step is less than the time to concentration for the modeled watershed. With longer landscape evolution time steps the model simulates a steady state regime."

Comment Table 2: this is only a partial list of codes that have been published in, say, the last ten years. Why choose these particular ones?

Response We removed the table and instead list or briefly discuss these landscape evolution models and others in the body of the Introduction.

Comment Table 2: Be careful about giving the spatial scale for these models. At least some of these codes have been used and published at a variety of different spatial scales, from say the size of a rilled hillslope to that of a small country; and in some cases (e.g., SIBERIA) is sometimes presented in a dimensionless mode in which no spatial scale at all is given or implied. As to temporal scale, I thought that at least some of these can also be run in 'event' mode. Also, my understanding is that Landlab is not itself a model, but rather is a programming library that contains components that can be used to build various types of model, including landscape evolution. That said, people seem to have built landscape evolution models using Landlab (the Landlab website lists some of these). Maybe it would make sense to label this entry as 'Landlab-built erosion models' or something like that.

Response We removed the table and instead list or briefly discuss these libraries and landscape evolution models in the text.

Comment Section 2.1 generally: I like the way that this is carefully organised into sub-sections. However, the order of presentation confused me. Often, authors presenting a set of governing equations will start with the high-level conservation law(s), and then define each term more precisely. As noted below, there's an opportunity to do this at least partly in subsection 2.1.1.

Response We agree and we have started this description with the general equation for change in elevation (continuous form of eq. 7) followed by general equation for d_s. See e.g. eq. (9) in Mitasova et al. 2005 ($D(r,t)$ is our d_s).

Comment Equation 2: it would be helpful to give some context and referencing. I think this idea comes from Foster and Meyer (1972), right? If I remember correctly, their key assumption was that the ratio of transport rate to transport capacity, plus the ratio of detachment rate to detachment capacity, sum to unity. Assuming I did the math right, this leads to a first-order reaction-like equation: $dz/dt = ds = sigma(qs - Tc)$ I recommend presenting it this way here in section 2.1.1 (in addition to the definition given in eq 2), because this relates transport and detachment to the rate of change of elevation, and motivates the need for definitions for qs, Tc, and Dc. Note that there seems to be a problem with units in one of the factors in eq 2: if Tc and

Dc had the same units (as is listed), then sigma would be dimensionless. I suspect Dc is actually in $kgm^{-2}s^{-1}$ (detached mass per unit area per time).

Response We have added a more complete explanation of the Foster and Meyer relationship and the related parameters and fixed the units for D_c (eq. 12-13 in Mitasova et al. 2005).

Comment Equation 4: symbol v is used without being introduced. Presumably it is the depth averaged flow velocity vector in (x,y). Either define v or use q (which you've defined already).

Response We modified the equation according to the reviewer's suggestion.

Comment Also, whereas the paper is premised on the value of having a dynamic representation of surface-water hydrology (which eq 3 is), equation 4 is actually a steady solution, is it not? If the model indeed uses a fully time-varying flow model, the equations presented in this sub-section should show this. In addition, it would be helpful to provide a reference for this form of the diffusion-wave approximation (could be to a hydrology text that gives the derivation and assumptions).

Response The in-depth explanation of mathematical foundations for the shallow water flow simulation has been addressed in several previously published papers, for example Mitasova et al. 2005, and we tried to avoid repeating text presented there, unfortunately this makes some of the concepts and reasoning behind the methods less clear. Therefore, we have rewritten the entire section 2 including more detailed explanation of the method and more specific references.

Comment "Please give units of epsilon."

Response Units for epsilon are now given in the text.

Comment 8/10 suggest specifying '...density in the water column', so it is clear that this is a mass concentration rather than a bulk density of resting sediment.

Response Changed as recommended by reviewer.

Comment 8/15 "steady state sediment flow with diffusion" - I'm confused by this. The equation is time-dependent, so how is it steady state? And the definition of qs above is advective, not diffusive.

Response We added the equation with diffusion term used in the path sampling solution, see e.g. Mitasova et al. 2005 eq. 16.

Comment 8/17 So we need a definition for ds, which as suggested above, you could provide in section 2.1.1.

Response Agreed. We rewrote section 2.1 and included a definition of ds.

Comment 8/23 In the previous equation, you used a continuum formulation, whereas here you're giving a discretized-in-time form. Please be consistent. I suggest sticking with continuum forms, because these don't require you to make any statements about numerical approximation. And in fact, as noted above, I recommend putting equation 7 in section 2.1.1.

Response We have rewritten the equation into continuum form and moved section 2.1.5 to section 2.1.1 following the reviewer's recommendation.

Comment Equation 8: this equation is not dimensionally consistent. If you write it in continuum form, $dz/dt = -(1/rho)qs$ you have m/s on the left and m2/s on the right. I'm also not convinced that the equation expresses the idea you want. I'm guessing that a detachment-limited regime would look more like $dz/dt = -(1/rho)Dc$. Then it becomes a question of what is your detachment capacity law? You've already introduced detachment capacity in $Dc = sigmaTc$ (eq 2). In order to close the equations, you need either a definition of Dc or Tc. Presumably these depend in some fashion on water discharge or velocity or boundary shear stress. Please specify (or, if I have misunderstood, explain why the equation set given is sufficient to describe the SIMWE module). Actually, after reading farther in the manuscript, I think the idea is that the RUSLE equation can be used for Dc in detachment-limited mode. If that's correct, then say something to the effect that the definition of Dc will be given in section so-and-so, and then use the symbol Dc in that section. Regarding the role of qs, I suspect what you're after is the notion that qs is the upstream/upslope integral of ds, is that right? If so, it would be helpful to present the math.

Response You are correct, using q_s here was an oversight. Eq. 8 is not really needed, because d_s in DLC is erosion rate given by eq 13 which is detachment rate (soil loss) not sediment flow. We have removed this equation.

Comment 9/21 please give the functional form of this relationship.

Response The equation for this relationship is given in the section 2.2.3.

Comment 10/2 I get that there's a long tradition of practical empiricism in soil-erosion research. But what about pushing ever so gently back on it by presenting equation 10 in a slightly less brutally ugly form? Something like: $er/e_ref = 1 - aexp(-ir/i_ref)$ where e_ref is reference energy equal to ... and i_ref is reference rainfall intensity equal to.

Response Thank you for the suggestion. We have modified the equation accordingly.

Comment "10/7 shouldn't this be rainfall depth rather than volume? Equation 11: again the units seem to be off here (apart from the oddity of having an 'index' that has [weird] units). I get the right side as being: $MJha^{-1}mm^{-1}xmmxs = MJha^{-1}s$?"

Response We have revised this equation, checked the units, and introduced it with Equation 2 from Panagos et al. 2015 from which it is derived.

Comment 11/3 the subsection is called 'Sediment flow' but it reads like an erosion rate. Though I guess it works given that you're defining it as mass flow per time per area.

Response You are right – it is an erosion rate (soil loss: mass per area per time). In this paper we were using the term sediment flow for sediment flow per unit width mass per length per time). We have retitled this subsection as Detachment Limited Erosion Rate and replaced sediment flow with erosion rate throughout the paper for this case.

Comment Equation 13: again I'm struggling with units. I get: $(MJmmha^{-1}hr^{-1})x(tonhahrha^{-1}MJ^{-1}mm^{-1}) = (ha^{-1})x(ton)$ which are not the units given for E.

Response We have revised the units for E and R.

Comment 11/16-17 it's not clear to me how these equations relate. Maybe you mean that the definition of E in equation 13 is the SAME AS ds (or -ds) for transport-limited conditions, and Dc for detachment-limited conditions? In that case, it might suffice to simply call equation 13 the definition of Dc. You could then give the definition of Tc as sigma = Dc/Tc ==> Tc = Dc/sigma (Note: it would be more intuitive to think in terms of a length scale, L = 1 / sigma, which is then the characteristic distance over which steady, uniform overland flow reaches its carrying capacity on a planar slope).

Response We have renamed this section and revised the text following the reviewer suggestion. The equation 8 was removed (see the related answer above).

Comment 11/29 not clear to me what 'topographic component of overland flow' means.

Response We revised section 2.4.1 "Topographic sediment transport factor".

Comment Equation 15: is T the same as T_c? Also, again, I'm not sure the units are correct here, please check, and correct if necessary.

Response Yes, T is T_c. We have unified the symbols and checked the units.

Comment Figures 5 and 6: why the different color schemes in two of the three comparisons (top and bottom rows)?

Response We have redone these figures (now 7-9). The subfigures showing the net difference may appear different, but have the same color table. Since the detachment limited regime only has negative values, the upper range of the color table does not appear.

Comment Figure 6: if the figure is meant to compare runs with two different rainfall intensities, which intensity was used for the upper and middle figures?

Response We have completely redone these figures, removed SIMWE's detachment and transport limited cases, and laid out the figures for more direct comparison.

Comment Software: I tested the model software by installing the latest stable release of GRASS GIS, then going to the GitHub repository for the model's source code. By following the "Basic Instructions" listed there, I was able to install the r.sim.terrain extension and run the example.

r.sim.terrain 1.0: a [..*]landscape evolution model with dynamic hydrology

Brendan Alexander Harmon[1], Helena Mitasova[2,3], Anna Petrasova[2,3], and Vaclav Petras[2,3]

[1]Robert Reich School of Landscape Architecture, Louisiana State University, Baton Rouge, Louisiana, USA
[2]Center for Geospatial Analytics, North Carolina State University, Raleigh, North Carolina, USA
[3]Department of Marine, Earth, and Atmospheric Sciences, North Carolina State University, Raleigh, North Carolina, USA

Correspondence: Brendan Harmon (baharmon@lsu.edu)

Abstract. While there are numerical landscape evolution models that simulate how steady state flows of water and sediment reshape topography over long periods of time, r.sim.terrain is the first to simulate short-term topographic change for both steady state and dynamic flow regimes across a range of spatial scales. This free and open source, GIS-based topographic evolution model uses empirical models for soil erosion [..[2]]and a physics-based model for shallow overland water flow and soil erosion [..[3]]to compute short-term topographic change. This [..[4]]model uses either a steady state or [..[5]]unsteady representation of overland flow to simulate how overland sediment mass flows reshape topography for a range of hydrologic soil erosion regimes based on topographic, land cover, soil, and rainfall parameters. As demonstrated by a case study for Patterson Branch subwatershed on the Fort Bragg military installation in North Carolina, r.sim.terrain [..[6]]simulates the development of fine-scale morphological features including ephemeral gullies, rills, and hillslopes. Applications include land management, erosion control, landscape planning, and landscape restoration.

1 Introduction

Landscape evolution models represent how the surface of the earth changes over time in response to physical processes. Most studies of landscape evolution have been descriptive, but a number of numerical landscape evolution models have been developed that simulate elevational change over time [..[15]](Tucker and Hancock, 2010; Temme et al., 2013). Numerical landscape evolution models such as the Geomorphic - Orogenic Landscape Evolution Model (GOLEM) (Tucker and Slinger-

---

*removed: dynamic

[2] removed: at watershed to regional scales

[3] removed: at subwatershed scales

[4] removed: either

[5] removed: dynamic model simulates

[6] removed: can realistically simulate

[15] removed: (Temme et al., 2013)

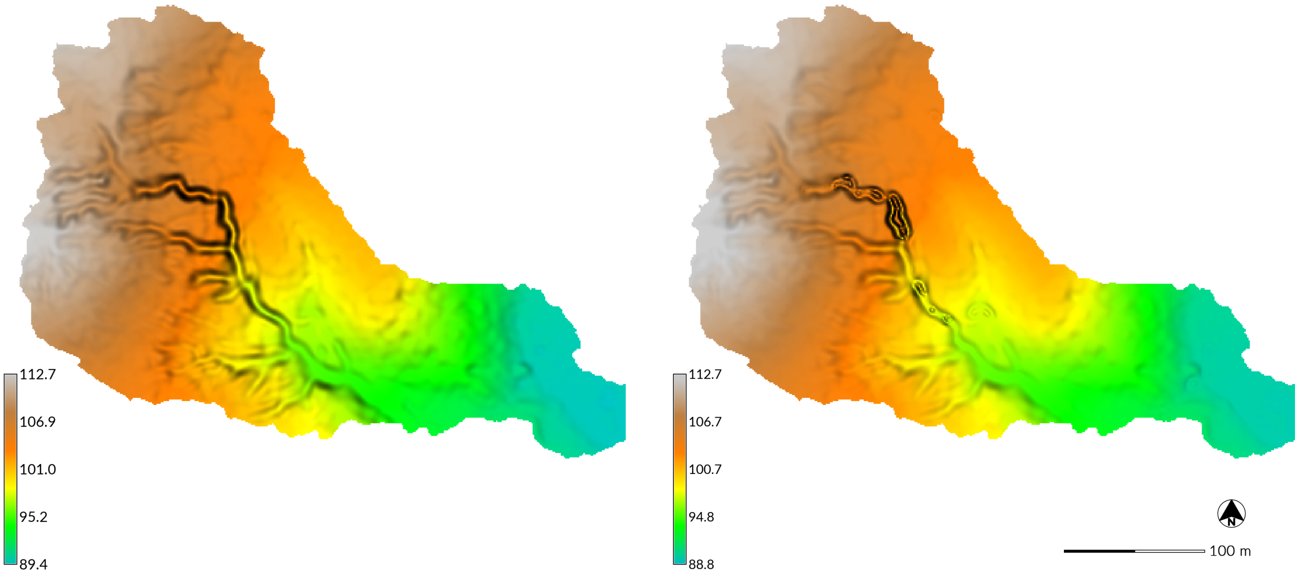

a.

b.

Figure 1. The digital elevation model (DEM) [..[7]](a[..[8]]) before and [..[9]](b[..[10]]) after simulated landscape evolution with r.sim.terrain for a subwatershed of Patterson Branch, Fort Bragg, NC, USA. (a) The before DEM was generated from an airborne lidar survey in 2012. This simulation used the SIMWE model for a $120\,\mathrm{min}$ rainfall event with [..[11]]$50\,\mathrm{mm\,hr^{-1}}$ [..[12]]for a [..[13]]variable erosion-deposition regime at steady state. (b) In the evolved DEM [..[14]]the gully channel has widened with depositional ridges forming along its thalweg.

land, 1994), CASCADE (Braun and Sambridge, 1997), the Channel-Hillslope Integrated Landscape Development (CHILD) model (Tucker et al., 2001)[..[16]], CAESAR (Coulthard et al., 2002, 2012), SIBERIA (Willgoose, 2005), LAPSUS (Schoorl et al., 2000, 2002), and r.landscape.evol (Barton et al., 2010) simulate landscape evolution driven primarily by steady state flows over long temporal scales. Landlab, a new Python library for numerically modeling Earth surface processes (Hobley et al., 2017), has components for simulating landscape evolution such as the Stream Power with Alluvium Conservation and Entrainment (SPACE) model (Shobe et al., 2017). While Geographic Information Systems (GIS) support efficient data management, spatial and statistical modeling and analysis, and visualization, there are few GIS-based soil erosion models (see Table 1) or landscape evolution models[..[17]]. Thaxton (2004) developed the model r.terradyn as a GRASS GIS shell script module to simulate terrain evolution by steady-state net erosion deposition rates estimated by the Simulation of Water Erosion (SIMWE) model (Mitas and Mitasova, 1998) and gravitational diffusion. Barton et al. (2010) developed a long term landscape evolution model in GRASS GIS called r.landscape.evol that integrates the Unit Stream Power Erosion Deposition (USPED) model, fluvial erosion, and gravitational diffusion. r.landscape.evol has been used to simulate the

---

[16] removed: and SIBERIA (Willgoose, 2005)simulate

[17] removed: (see Tables 1-**??**)

impact of prehistoric settlements on Mediterranean landscapes. [..[18]]In spite of the recent progress in landscape evolution modeling and monitoring, there are still major research questions to address in the theoretical foundations of erosion modeling such as how erosional processes scale over time and space and how sediment detachment and transport interact (Mitasova et al., 2013). While most numerical landscape evolution models simulate [..[19]]erosion processes at steady state[..[20]], peak flows short-term erosional processes like gully formation can be [..[21]]driven by unsteady, dynamic flow with significant morphological changes happening [..[22]]before flows reach steady state. A [..[23]]landscape evolution model with dynamic water and sediment flow is needed to study fine-scale spatial and short-term temporal erosional processes such as gully formation and the development of microtopography.

At the beginning of a rainfall event the overland water flow [..[24]]is unsteady – its depth changes at a variable rate over time and space. If the intensity of rainfall continues to change throughout the event then the flow regime will remain dynamic. If, however, the overland flow reaches a peak rate then the hydrologic regime is considered to be at steady state. At steady state:

$$\frac{\partial h(x,y,t)}{\partial t} = 0 \tag{1}$$

where:

(x,y) is the position $[\mathrm{m}]$

t is the time $[\mathrm{s}]$

$h(x,y,t)$ is the depth of overland flow $[\mathrm{m}]$

Gullies are eroded, steep banked channels formed by ephemeral, concentrated flows of water. A gully forms when overland waterflow converges in a knickzone – a concave space with steeper slopes than its surroundings (Zahra et al., 2017) – during intense rainfall events. When the force of the water flow concentrated in the knickzone is enough to detach and transport large amounts of sediment, an incision begins to form at the apex of the knickzone – the knickpoint or headwall. As erosion continues the knickpoint begins to migrate upslope and the nascent gully channel widens, forming steep channel banks. Multiple incisions initiated by different knickpoints may merge into a gully channel and multiple channels may merge into a branching gully system (Mitasova et al., 2013). This erosive process is dynamic; the morphological changes drive further changes in a positive feedback loop[..[25]]. When the gully initially forms the soil erosion regime should be detachment capacity limited with the concentrated flow of water in the channel of the gully detaching large amounts of sediment and transporting it to the foot of the gully, potentially forming a depositional fan. [..[26]]If the intensity of rainfall decreases and transport and detachment

---

[18] removed: Furthermore

[19] removed: peak flows

[20] removed: (see Table **??**),

[21] removed: dynamic

[22] removed: within minutes

[23] removed: dynamic

[24] removed: regime is dynamic

[25] removed: until water flow reaches steady state

[26] removed: After the initial formation of the gully

capacity approach a balance, then the soil erosion regime may switch to a variable erosion-deposition [..[27]]regime, in which soil is eroded and deposited in a spatially variable pattern. Subsequent rainfall events may trigger further knickpoint formation and upslope migration, channel incision and widening, and depositional fan and ridge formation. Between high intensity rainfall events, lower intensity events and gravitational diffusion may gradually smooth the shape of the gully. Eventually, if detachment capacity significantly exceeds transport capacity and the regime switches to transport capacity limited, the gully may fill with sediment, as soil continues to be eroded, but is not transported far.

Gully erosion rates and evolution can be monitored in the field or modeled on the computer. Field methods include dendrogeomorphology (Malik, 2008) and permanent monitoring stakes for recording erosion rates, extensometers for recording mass wasting events, weirs for recording water and suspended sediment discharge rates, and time series of surveys using total station theodolites (Thomas et al., 2004), unmanned aerial systems (UAS) (Jeziorska et al., 2016; Kasprak et al., 2019; Yang et al., 2019), airborne lidar (Perroy et al., 2010; Starek et al., 2011), and terrestrial lidar [..[28]](Starek et al., 2011; Bechet et al., 2016; Goodwin et al., 2016; Telling et al., 2017). With terrestrial lidar, airborne lidar, and UAS photogrammetry there is now sufficient resolution topographic data to morphometrically analyze and numerically model fine-scale landscape evolution in GIS including processes such as gully formation and the development of microtopography. Gully erosion has been simulated with [..[29]]RUSLE2-Raster (RUSLER) in conjunction with the Ephemeral Gully Erosion Estimator (EphGEE) (Dabney et al., 2014), while gully evolution has been simulated for detachment capacity limited erosion regimes with the Simulation of Water Erosion (SIMWE) model (Koco, 2011; Mitasova et al., 2013). Now numerical landscape evolution models that can simulate steady state and [..[30]]unsteady flow regimes and [..[31]]dynamically switch between soil erosion regimes are needed to study fine-scale spatial and short-term [..[32]]erosional processes.

The numerical landscape evolution model r.sim.terrain was developed to simulate the spatiotemporal evolution of landforms caused by shallow overland water and sediment flows at spatial scales ranging from square meters to kilometers and temporal scales ranging from minutes to years. This open source, GIS-based landscape evolution model can simulate either steady state or [..[33]]unsteady flow regimes, dynamically switch between soil erosion regimes, and simulate the evolution of fine-scale morphological features such as ephemeral gullies (Figure 2). It was designed as a research tool for studying how erosional processes scale over time and space, comparing empirical and process-based models, comparing steady state and [..[34]]unsteady flow regimes, and studying the role of [..[35]]unsteady flow regimes in fine-scale morphological change. r.sim.terrain was tested with a subwatershed scale (450 m^2) case study and the simulations were compared against a time-series of airborne lidar surveys.

---

[27] removed: if the intensity of rainfall decreases

[28] removed: (Starek et al., 2011; Bechet et al., 2016)

[29] removed: the Revised Universal Soil Loss Equation Version 2

[30] removed: dynamic

[31] removed: can

[32] removed: temporal

[33] removed: dynamic

[34] removed: dynamic

[35] removed: dynamic

2 r.sim.terrain

The process-based, spatially distributed landscape evolution model r.sim.terrain simulates topographic changes caused by shallow, overland water flow across a range of spatiotemporal scales and soil erosion regimes using either the Simulated Water Erosion (SIMWE) model, the 3-Dimensional Revised Universal Soil Loss Equation (RUSLE 3D) model, or the Unit Stream Power Erosion Deposition (USPED) model (2). The r.sim.terrain model can simulate either steady state or dynamic flow regimes. SIMWE is a physics-based simulation that uses a Monte Carlo path sampling method to solve the water and sediment flow equations for detachment limited, transport limited, and variable erosion-deposition soil erosion regimes [..[36]](Mitas and Mitasova, 1998; Mitasova et al., 2004). With SIMWE r.sim.terrain uses the modeled flow of sediment – a function of water flow and soil detachment and transport parameters – to estimate net erosion and deposition rates. RUSLE3D is an empirical equation for [..[37]]estimating soil erosion rates in detachment capacity limited soil erosion regimes [..[38]](Mitasova et al., 1996, 2013). With RUSLE3D r.sim.terrain uses an event-based rainfall erosivity factor, [..[39]]soil erodibility factor, landcover factor, and 3D topographic factor [..[40]]– a function of slope and flow accumulation – to model soil erosion rates. USPED is [..[41]]a semi-empirical equation for net erosion and deposition in transport capacity limited soil erosion regimes (Mitasova et al., 1996, 2013). With USPED r.sim.terrain uses an event-based rainfall erosivity factor, [..[42]]soil erodibility factor, landcover factor, and a 3D topographic factor to model [..[43]]net erosion or deposition rates as the divergence of sediment [..[44]]flow. For each of the models topographic change is derived at each time step from the [..[45]]net erosion-deposition rate and gravitational diffusion. [..[46]]Depending on the input parameters, r.sim.terrain [..[47]]simulations with SIMWE [..[48]]can represent variable soil erosion-deposition [..[49]]regimes, including prevailing detachment capacity limited or prevailing transport capacity limited regimes.

The r.sim.terrain model can simulate the evolution of gullies including processes such as knickpoint migration, channel incision, channel widening, aggradation, and scour pool and depositional ridge formation along the thalweg of the gully. Applications include geomorphological research, erosion control, landscape restoration, and scenario development for landscape planning and management. This model can simulate landscape evolution over a wide range of spatial scales from small watersheds less than ten square kilometers with SIMWE to regional watersheds of hundreds of square kilometers with USPED or RULSE3D, although it does not model fluvial processes. It has been used at resolutions ranging from

---

[36] removed: (Mitasova et al., 2004)

[37] removed: sediment flows

[38] removed: (Mitasova et al., 1996).

[39] removed: the slope, the flow accumulation, and a

[40] removed: to model sediment flow

[41] removed: an empirical

[42] removed: the slope and aspect, the flow accumulation

[43] removed: erosion-deposition as the the

[44] removed: flows

[45] removed: sediment flow or

[46] removed: The

[47] removed: model can simulate either steady state or dynamic flow regimes. During

[48] removed: r.sim.terrain can switch between detachment limited, transport limited, and variable

[49] removed: soil erosion

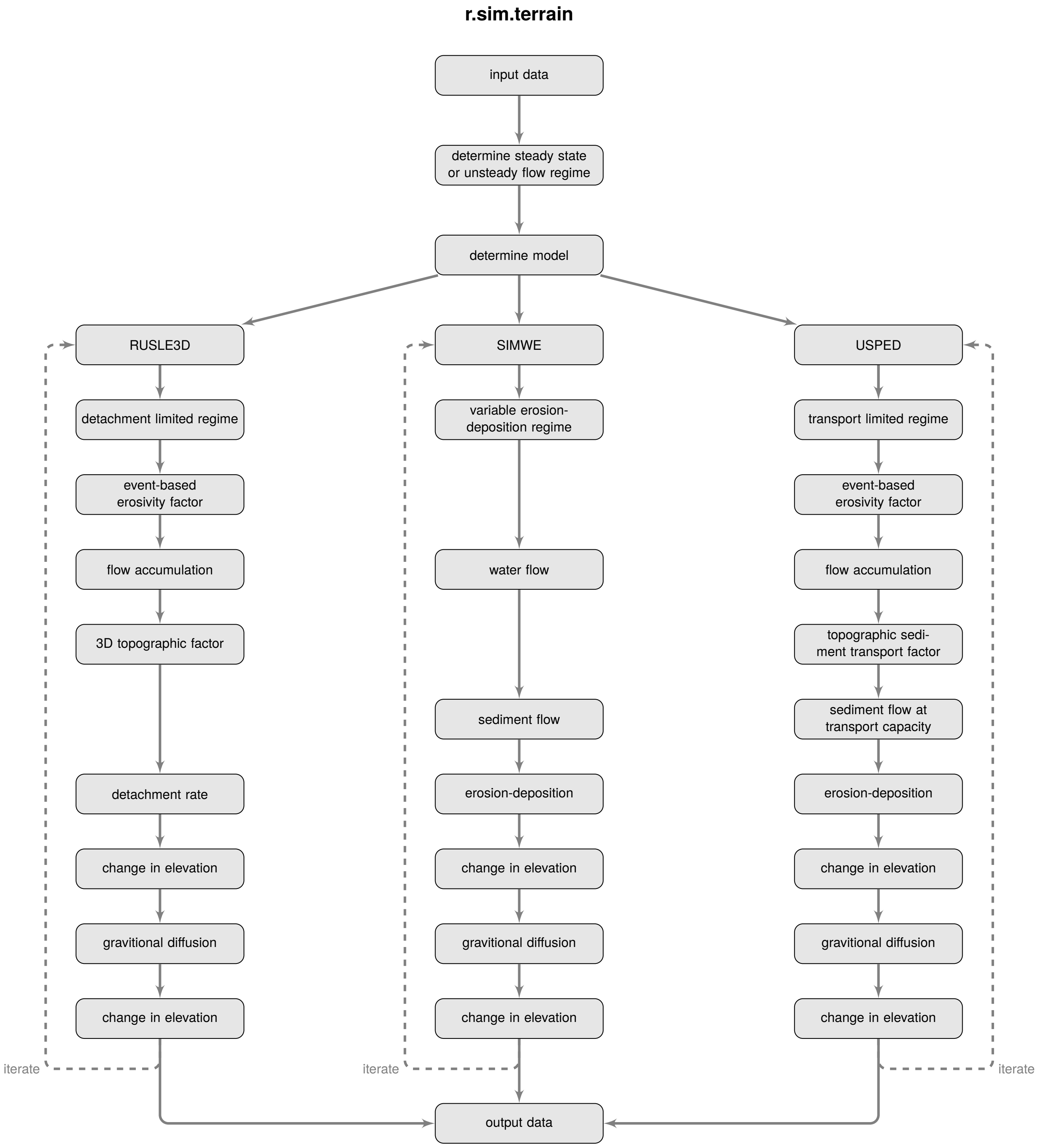

Figure 2. Conceptual diagram for r.sim.terrain.

Table 1. Geospatial soil erosion models

Model	Spatial scale	Temporal scale	Representation	Implementation	Reference
RUSLE3D	regional	continuous	raster	map algebra	(Mitasova et al., 1996)
USPED	watershed	continuous	raster	map algebra	(Mitasova et al., 1996)
SIMWE	watershed	event – continuous	raster	GRASS modules	(Mitas and Mitasova, 1998)
GeoWEPP	watershed	continuous	raster	ArcGIS module	(Flanagan et al., 2013)
AGWA	watershed	event – continuous	vector	ArcGIS module	(Guertin et al., 2015)
openLISEM	watershed	event	raster	PCRaster script	(Roo et al., 1996)
Landlab	watershed	event – continuous	raster + mesh	Python library	(Hobley et al., 2017)

sub-meter to 30 m. [..[50]]The model has been implemented as a Python add-on module for the free, open source Geographic Resources Analysis Support System (GRASS) GIS (GRASS Development Team). The source code is available at https://github.com/baharmon/landscape_evolution under the GNU General Public License v2. It supports multithreading and parallel processing to efficiently compute simulations using large, high resolution topographic datasets. The landscape evolution model can be installed in GRASS GIS as an add-on module with the command:

```
g.extension extension=r.sim.terrain
```

2.1 [..[52]]Landscape evolution

Landscape evolution in r.sim.terrain is driven by the change in the elevation surface caused by soil erosion and deposition. During storm events overland flow erodes soil, transports sediment across landscape, and under favorable conditions deposits the sediment. Gravitational diffusion, applied to the changed elevation surface, simulates the smoothing effects of localized soil transport between events.

2.1.1 Elevation change

Assuming negligible uplift, the change in elevation over time is described by the continuity of mass equation expressed as the divergence of sediment flow (Tucker et al., 2001):

$$\frac{\partial z}{\partial t} = \left(-\nabla \cdot \mathbf{q_s} i\right)\ \rho_s^{-1} = d_s\ \rho_s^{-1} \tag{2}$$

---

[50] removed: This

[52] removed: Simulation of water erosion model

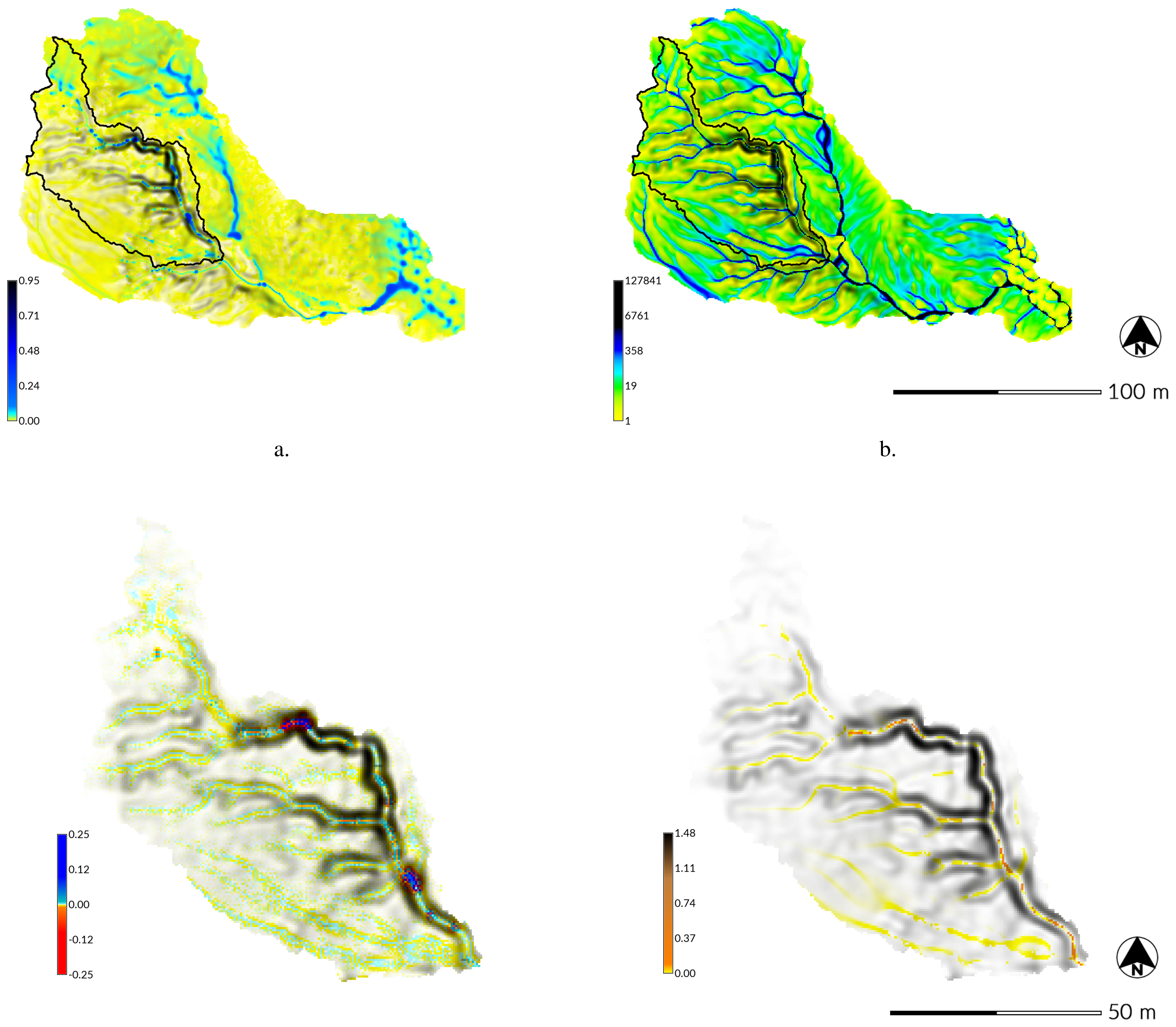

a.

b.

c.

d.

Figure 3. Water and sediment flows modeled by (a & c) SIMWE and (b & d) RUSLE3D with spatially variable landcover for a (a & b) subwatershed and (c & d) drainage area of Patterson Branch, Fort Bragg, NC. (a) Water depth $[\mathrm{m}]$ simulated by SIMWE for a $10\ \mathrm{min}$ event with $50\ \mathrm{mm\,hr^{-1}}$ in the subwatershed. (b) Flow accumulation for RUSLE3D in the subwatershed. (c) Erosion and deposition $[\mathrm{kg\,m^{-2}\,s^{-1}}]$ simulated by SIMWE in drainage area 1. (d) Erosion $[\mathrm{kg\,m^{-2}\,s^{-1}}]$ modeled by RUSLE3D [..51]in drainage area 1.

where:

z is elevation $[\mathrm{m}]$

t is time $[\mathrm{s}]$

$\mathbf{q_s}$ is sediment flow per unit width (vector) $[\mathrm{kg\,m^{-1}\,s^{-1}}]$

d_s is the net erosion-deposition rate $[\mathrm{kg\,m^{-2}\,s^{-1}}]$

ρ_s is sediment mass density $[\mathrm{kg\,m^{-3}}]$.

The net erosion-deposition rate d_s driven by overland flow in r.sim.terrain is estimated at different levels of complexity based on the simulation mode selected by the user. Gravitational diffusion is then applied to the changed topography to simulate the smoothing effects of localized soil transport between rainfall events. The change in elevation due to gravitational diffusion is a function of the sediment mass density, the diffusion coefficient, and Laplacian of the elevation (Thaxton, 2004):

$$\frac{\partial \mathrm{z}}{\partial \mathrm{t}} = \rho_{\mathrm{s}}^{-1}\,\varepsilon_{\mathrm{g}}\,\nabla^2 \mathrm{z} \tag{3}$$

where ε_g is the diffusion coefficient $[\mathrm{kg\,m^{2}\,s^{-1}}]$.

The discrete implementation follows Thaxton (2004):

$$\mathrm{z}_{\mathrm{t}+\Delta \mathrm{t}_1} = \mathrm{z}_{\mathrm{t}} + \Delta \mathrm{z}_{\mathrm{s}} \tag{4}$$

$$z_{t+\Delta t_1+\Delta t_2} = z_{t+\Delta t_1} + \Delta z_g \tag{5}$$

where:

Δz_s is elevation change caused by net erosion or deposition $[\mathrm{m}]$ (Eq. 2)

Δz_g is the diffusion driven elevation change $[\mathrm{m}]$ (Eq. 3)

Δt_1 is the time interval during a storm event $[\mathrm{s}]$

Δt_2 is the time interval between events when gravitational diffusion changes the elevation surface $[\mathrm{s}]$.

2.1.2 Erosion-deposition regimes

Following experimental observations and qualitative arguments, Foster et al. (1977) proposed that the sum of the ratio of the net erosion-deposition rate d_s to detachment capacity D_c $[\mathrm{kg\,m^{-2}\,s^{-1}}]$ and the ratio of the sediment flow rate $q_s = |\mathbf{q_s}|$ to sediment transport capacity T_c $[kg\ m^{-1}\ s^{-1}]$ is a conserved quantity (unity):

$$\frac{\mathrm{d_s}}{\mathrm{D_c}} + \frac{\mathrm{q_s}}{\mathrm{T_c}} = 1 \tag{6}$$

The net erosion and deposition rate d_s can then be expressed as being proportional to the difference between the sediment transport capacity T_c and the actual sediment flow rate q_s:

$$\mathrm{d_s} = \frac{\mathrm{D_c}}{\mathrm{T_c}}\left(\mathrm{T_c} - \mathrm{q_s}\right) \tag{7}$$

This principle is used in several erosion models including the Water Erosion Prediction Project (WEPP) (Flanagan et al., 2013) and SIMWE (Mitas and Mitasova, 1998).

Using this concept it is possible to identify two limiting erosion-deposition regimes. When $T_c >> D_c$ leading to $T_c >> q_s$, the erosion regime is detachment capacity limited and net erosion is equal to the detachment capacity:

$$\mathrm{d_s} = \mathrm{D_c} \tag{8}$$

For this case the transport capacity of overland flow exceeds the detachment capacity and thus sediment flow, erosion, and sediment transport are limited by the detachment capacity. Therefore, no deposition occurs. An example of this case is when a strong storm producing intense overland flow over compacted clay soils causes high capacity flows to transport light clay particles, while the detachment of compacted soils is limited. When $D_c >> T_c$, sediment flow is at sediment transport capacity $q_s = T_c$, leading to a transport capacity limited regime with deposition reaching its maximum extent for the given water flow. Net erosion-deposition is computed as the divergence of transport capacity multiplied by a unit vector $\boldsymbol{s_0}$ in the direction of flow:

$$\mathrm{d_s} = \nabla \cdot (\mathrm{T_c}\ \boldsymbol{s_0}) \tag{9}$$

This case may occur, for example, during a moderate storm with overland flow over sandy soils with high detachment capacity, but low transport capacity. For $0 < (D_c/T_c) < \infty$ the spatial pattern of net erosion-deposition is variable and depends on the difference between the sediment transport capacity and the actual sediment flow rate at the given location.

The detachment capacity D_c and the sediment-transport capacity T_c are estimated using shear stress and stream power equations respectively expressed as power functions of water-flow properties and slope angle. The relation between the topographic parameters of well known empirical equations for erosion modeling, such as USLE and stream power, were presented by (Moore and Burch, 1986) and used to develop simple, GIS-based models for limiting erosion-deposition cases such as RUSLE3D and USPED (Mitasova and Mitas, 2001). The SIMWE model estimates T_c and D_c using modified equations and parameters developed for the WEPP model (Flanagan et al., 2013; Mitasova and Mitas, 2001).

The simulation modes in r.sim.terrain include:

- the process-based SIMWE model for steady state and unsteady shallow overland flow in variable erosion-deposition regimes with d_s computed by solving the shallow water flow and sediment transport continuity equations,
- the RUSLE3D model for detachment capacity limited cases with d_s given by Eq. (8),
- and the USPED model for transport capacity limited regimes with d_s given by Eq. (9).

The following sections explain the computation of d_s for these three modes in more detail.

2.2 Simulation of Water Erosion (SIMWE)

SIMWE [..[53]]is a physics-based simulation of shallow overland water and sediment flow that uses a path sampling method to solve the continuity [..[54]]equations with a 2D diffusive wave approximation (Mitas and Mitasova, 1998; Mitasova et al., 2004). SIMWE has been implemented in GRASS GIS as the modules r.sim.water and r.sim.sediment.

In SIMWE mode for each landscape evolution time step r.sim.terrain[..[55]]:

- computes the first order partial derivatives of the [..[56]]elevation surface $\partial z/\partial x$ and $\partial z/\partial y$,
- simulates shallow water flow [..[57]]depth, sediment flow, and the net erosion-deposition [..[58]]rate,
- and then evolves the topography based on the erosion-deposition rate and gravitational diffusion. [..[59]]

The first order partial derivatives of the [..[60]]elevation surface are computed using the GRASS GIS module r.slope.aspect using the equations in Hofierka et al. (2009). r.sim.terrain simulates unsteady-state flow regimes when the landscape evolution time step is less than the travel time for a drop of water or a particle of sediment to cross the landscape, e.g. when the time step is less than the time to concentration for the modeled watershed. With longer landscape evolution time steps the model simulates [..[61]]

2.2.1 [..[62]]

[..[63]]

$$\sigma = \frac{D_c}{T_c}$$

---

[53] removed: – the Simulation of Water Erosion model –

[54] removed: and momentum

[55] removed: determines the soil erosion regime, simulates water and sediment flows, and then evolves the topography. In an variable erosion-deposition regime the model computes the

[56] removed: topography,

[57] removed: and

[58] removed: ,

[59] removed: The same process is used in a transport capacity limited regime, except that the topography is evolved based on the transport limited erosion-deposition rate and gravitational diffusion. In a detachment capacity limited regime the model instead computes the

[60] removed: topography, simulates shallow water flow and sediment flow, and then evolves the topography based on the sediment flow rate and gravitational diffusion. The model simulates dynamic landscape evolution when the

[61] removed: steady state dynamics.

[62] removed: Erosion regime

[63] removed: This model can switch erosion regimes at each time step based on the rainfall intensity (i_r) and the balance of the sediment detachment capacity (D_c) and the sediment transport capacity (T_c) represented by the first order reaction term σ, which depends on soil and landcover properties. The detachment capacity is the maximum potential detachment rate by overland flow, while the sediment transport capacity is the maximum potential sediment flow rate. When rainfall intensity is very high ($i_r \geq 60\mathrm{mm\,hr}^{-1}$) or σ is low ($\sigma \leq 0.01\mathrm{m}^{-1}$), then the regimeis detachment capacity limited. When rainfall intensity is not very high ($i_r < 60\mathrm{mm\,hr}^{-1}$) and σ is high ($\sigma \geq 100\mathrm{m}^{-1}$), then the regime is transport capacity limited. When rainfall intensity is not very high ($i_r < 60\mathrm{mm\,hr}^{-1}$) and σ is neither high nor low ($0.01\mathrm{m}^{-1} < \sigma < 100\mathrm{m}^{-1}$), then there is an variable erosion-deposition regime.

[..[64]]

[..[65]][[..[66]]]

[..[67]][[..[68]]]

[..[69]][[..[70]]]

a steady state regime.

2.2.1 Shallow water flow

The SIMWE model simulates shallow overland water flow controlled by spatially variable topographic, soil, landcover, and rainfall parameters by solving the [..[71]]water flow continuity equation using a Green's function Monte Carlo path sampling method[..[72]]:

$$\frac{\partial h}{\partial t} = i_e - \nabla\, q$$

[..[73]]

[..[74]][[..[75]]]

[..[76]][[..[77]]]

[..[78]][[..[79]]]

[..[80]][[..[81]]]

[..[82]]

[..[83]]

[..[84]][[..[85]]][..[86]]

---

[64] removed: where:

[65] removed: σ is a first order reaction term

[66] removed: m^{-1}

[67] removed: D_c is the sediment detachment capacity

[68] removed: $\mathrm{kg\,m}^{-1}s^{-1}$

[69] removed: T_c is the sediment transport capacity

[70] removed: $\mathrm{kg\,m}^{-1}s^{-1}$

[71] removed: continuity and momentum equations for steady state water flow with a

[72] removed: (Fig. 3a). Shallow water flow q can be approximated by the bivariate form of the St. Venant equation:

[73] removed: where:

[74] removed: x, y is the position

[75] removed: m

[76] removed: t is the time

[77] removed: s

[78] removed: h is the depth of overland flow

[79] removed: m

[80] removed: i_e is the rainfall excess

[81] removed: $\mathrm{m\,s}^{-1}$

[82] removed: (i.e. rainfall intensity − infiltration − vegetation intercept)

[83] removed: ∇ is the divergence of the flow vector field

[84] removed: q is the water flow per unit width

[85] removed: $\mathrm{m}^2\ \mathrm{s}^{-1}$

[86] removed: .

$$\nabla \cdot \boldsymbol{q} = i_e \tag{10}$$

where:

i_e is the rainfall excess rate $[\mathrm{m\,s^{-1}}]$ (i.e. rainfall intensity $-$ infiltration $-$ vegetation intercept)

$\boldsymbol{q}$ is the water flow per unit width (vector) $[\mathrm{m^2\ s^{-1}}]$.

[..[87]]The path sampling method solves the continuity equation through the accumulation of the evolving source over the given time period. This accumulation process can be interpreted as an approximation of a dynamic solution with diffusive wave effects incorporated by adding a diffusion term proportional to $\nabla^2[h^{5/3}]$ in the solution:

$$-\frac{\varepsilon_w}{2}\nabla^2\, h^{5/3} + \nabla \cdot \boldsymbol{q} = i_e \tag{11}$$

where:

ε_w is a spatially variable diffusion coefficient $[\mathrm{m^{4/3}\ s^{-1}}]$.

See Mitasova et al. (2004) for more details on this equation and its numerical solution. The solution assumes that water flow velocity is largely controlled by the slope of the terrain and surface roughness and that its change at a given location during the simulated event is negligible. The water depth h at time τ during the simulated rainfall event is computed as a function of particle (walkers) density at each grid cell. The initial number of particles per grid cell is proportional to the rainfall excess rate i_e (source). Particles are then routed across the landscape by finding a new position for each walker at time $\tau + \Delta\tau$:

$$\boldsymbol{r}_{\mathrm{m}}^{\mathrm{new}} = \boldsymbol{r}_{\mathrm{m}} + \Delta\tau\boldsymbol{v} + \boldsymbol{g} \tag{12}$$

where:

$\boldsymbol{r} = (x, y)$ is the m^{th} walker position [m]

$\Delta\tau$ is the particle routing time step [s]

$\boldsymbol{g}$ is a random vector with gaussian components with variance $\Delta\tau$ [m]

$\boldsymbol{v}$ is the water flow velocity vector $[\mathrm{m\,s^{-1}}]$ whose magnitude is computed with the Manning's equation $v = n^{-1}\ h^{2/3}\ s^{1/2}$ where n is the Manning's coefficient $[\mathrm{s\,m^{-1/3}}]$ and s is slope.

The mathematical background of the method, including the incorporation of approximate momentum through an increased diffusion rate in the prevailing direction of flow, is presented by Mitas and Mitasova (1998) and Mitasova et al. (2004).

2.2.2 Sediment flow and net erosion-deposition

The SIMWE model simulates the sediment flow over complex topography with spatially variable overland flow, soil, and landcover properties by solving the sediment flow continuity equation using a Green's function Monte Carlo path sampling

---

[87] removed: Diffusive wave effects can be approximated so that water can flow through depressions by integrating a diffusion term $\propto \nabla^2[h^{5/3}]$ into the solution of the continuity and momentum equations for steady state water flow . This equation is solved

method.

$$-\frac{\varepsilon}{2}\nabla^2[h^{5/3}] + \nabla\,[h\,v] = i_e$$

[..[88]]

[..[89]]

2.2.3 [..[90]]

[..[91]]Steady state sediment flow $\boldsymbol{q_s}$ is approximated by the bivariate continuity equation, which relates the change in sediment flow rate [..[92]]to effective sources and sinks:

$$\nabla \cdot \boldsymbol{q_s} = \text{sources} - \text{sinks} = \mathsf{d_s} \tag{13}$$

The sediment-flow rate $\boldsymbol{q_s}$ is a function of water flow and sediment concentration (Mitas and Mitasova, 1998)[..[93]]

$$q_s = \rho_s\, q$$

[..[94]]

[..[95]][[..[96]]]

[..[97]][[..[98]]][..[99]]

2.2.3 [..[100]]

[..[101]]:

$$d_s = \frac{\partial[\rho_s\, h]}{\partial t} + \nabla\, q_s$$

---

[88] removed: where:

[89] removed: ε is a spatially variable diffusion coefficient.

[90] removed: Sediment flow

[91] removed: In SIMWE the

[92] removed: q_s is estimated as

[93] removed: (Fig. 3b):

[94] removed: where:

[95] removed: q_s is the sediment flow rate per unit width

[96] removed: $\mathrm{kg\,m^{-1}\,s^{-1}}$

[97] removed: ρ_s is sediment mass density

[98] removed: $\mathrm{kg\,m^{-3}}$

[99] removed: .

[100] removed: Erosion-deposition

[101] removed: In SIMWE the net erosion-deposition rate is estimated using the bivariate form of sediment continuity equation to model sediment storage and flow based on effective sources and sinks (Fig. 3c). Net erosion-deposition d_s – the difference between sources and sinks – is approximated by the steady state sediment flow equationwith diffusion

[..[102]]

[..[103]][[..[104]]][..[105]]

$$\boldsymbol{q_s} = \rho_s \, c \, \boldsymbol{q} = \rho_s \, c \, h \, \boldsymbol{v} = \varrho \, \boldsymbol{v} \tag{14}$$

where:

ρ_s is sediment mass density in the water column $[\mathrm{kg\,m^{-3}}]$

c is sediment concentration $[\mathrm{particle\,m^{-3}}]$

$\varrho = \rho_s \, c \, h$ is the mass of sediment transported by water per unit area $[\mathrm{kg\,m^{-2}}]$.

2.2.3 [..[106]]

The sediment flow equation (13), like the water flow equation, has been rewritten to include a small diffusion term that is proportional to the mass of water-carried sediment per unit area $\nabla^2\varrho$ (Mitas and Mitasova, 1998):

$$-\frac{\varepsilon_s}{2}\nabla^2\varrho + \nabla\cdot[\varrho\boldsymbol{v}] + \varrho\,\frac{D_c}{T_c}\,|\mathbf{v}| = D_c \tag{15}$$

where:

ε_s is the diffusion constant $[\mathrm{m^2\,s^{-1}}]$.

[..[107]]On the left hand side of equation 15, the first term describes local diffusion, the second term is drift driven by the water flow, and the [..[108]] [..[109]]

third term represents a velocity dependent ‘potential’ acting on the mass of transported sediment. The initial number of particles per grid cell is proportional to the soil detachment capacity D_c (source). The particles are then routed across the landscape by finding a new position for each the walker at time $\tau + \Delta\tau$:

$$\boldsymbol{r}_{\mathrm{m}}^{\mathrm{new}} = \boldsymbol{r}_{\mathrm{m}} + \Delta\tau\boldsymbol{v} + \boldsymbol{g} \tag{16}$$

while the updated weight is:

$$w_m^{new} = w_m \exp[-\Delta\tau(u(\boldsymbol{r}_m^{new}) + u(\boldsymbol{r}_m))/2] \tag{17}$$

---

[102] removed: where:

[103] removed: d_s is net erosion-deposition

[104] removed: $\mathrm{kg\,m^{-2}\,s^{-1}}$

[105] removed: .

[106] removed: Landscape evolution

[107] removed: The simulated change in elevation Δz due to water erosion and deposition is a function of the change in time, the net erosion-deposition rate

[108] removed: sediment mass density (Mitasova et al., 2013):

[109] removed:

$$\Delta z = \Delta t \; d_s \; \rho_s^{-1}$$

where:

$u = D_c/T_c \; |\boldsymbol{v}|$.

[..[110]]The sediment flow rate [..[111]]

$$\Delta z = \Delta t \; q_s \; \varrho_s^{-1}$$

[..[112]]

[..[113]][[..[114]]][..[115]]

is computed as the product of weighted particle densities and the unit vector in the direction of flow $\boldsymbol{q_s} = \varrho \; \boldsymbol{s_0}$. Then net erosion-deposition d_s is computed as the divergence of sediment flow using equation (13).

SIMWE estimates the detachment capacity D_c and the sediment-transport capacity T_c as functions of shear stress and stream power respectively. Specifically, the detachment capacity is:

$$D_c = K_d \left(\gamma - \gamma_0\right)^b \tag{18}$$

where:

K_d is the effective erodibility (detachment-capacity coefficient) $[\mathrm{s\,m^{-1}}]$ for $b = 1$

$\gamma = \rho_w \; g \; h \; \sin\beta$ is shear stress $[\mathrm{Pa = kg\,m^{-2}}]$

ρ_w is the mass density of water $[\mathrm{kg\,m^{-3}}]$

g is gravitational acceleration $[\mathrm{m\,s^{-2}}]$

γ_0 is critical shear stress [Pa]

b is an empirical exponent.

[..[116]]Shear stress γ is computed as a function of water depth h estimated by r.sim.water and the surface slope angle β [°]. Sediment-transport capacity is computed as a function of [..[117]]unit stream power ω (Moore and Burch, 1986):

$$T_c = K_s \omega = K_s \; \gamma \; |\mathbf{v}| = K_s \; n^{-1} \; g_w \; h^m \; (\sin\beta)^p \tag{19}$$

where:

K_s is the effective sediment-transport capacity coefficient [s]

m and p are empirical exponents.

This model can simulate erosion regimes from prevailing detachment limited conditions when $T_c >> D_c$ to prevailing transport capacity limited conditions when $D_c >> T_c$ and the erosion-deposition patterns between these conditions.

---

[110] removed: In a detachment limited erosion regime the simulated change in elevation Δz is a function of the change in time , the

[111] removed: , and the mass of water carried sediment per unit area (Mitasova et al., 2013):

[112] removed: where:

[113] removed: ϱ_s is the mass of sediment per unit area

[114] removed: $\mathrm{kg\,m^{-2}}$

[115] removed: .

[116] removed: Gravitational diffusion is then applied to the evolved topography to simulate the settling of sediment particles.The simulated change in elevation Δz due to gravitational diffusion is

[117] removed: the change in time , the sediment mass density, the gravitational diffusion coefficient, and topographic divergence –

At each landscape evolution time step, the regime can change based on the ratio between the sediment detachment capacity D_c and the sediment transport capacity T_c and the actual sediment flow rate. If the landscape evolution time step is shorter than the time to concentration (i.e. the [..[118]]

$$\Delta z = \Delta t\, \rho_s^{-1}\, \varepsilon_g\, \nabla$$

[..[119]]

[..[120]][[..[121]]]

[..[122]][[..[123]]][..[124]]

time for water to reach steady state) then net erosion-deposition is derived from unsteady flow.

2.3 Revised [..[125]]Universal Soil Loss Equation for Complex Terrain (RUSLE3D)

[..[126]]RUSLE3D [..[127]]is an empirical [..[128]]model for computing erosion in a detachment capacity limited soil erosion regime for watersheds with complex topography (Mitasova et al., 1996). It is based on the Universal Soil Loss Equation (USLE), an empirical equation for estimating the average sheet and rill soil erosion from rainfall and runoff on agricultural fields and rangelands with simple topography (Wischmeier et al., 1978). It models erosion dominated regimes without deposition in which sediment transport capacity is uniformly greater than detachment capacity. [..[129]]In USLE soil loss per unit area is determined by an erosivity factor R, a soil erodibility factor K, a slope length factor L, a slope steepness factor S, a cover management factor C, and a prevention measures factor P. These factors are empirical constants derived from an extensive collection of measurements on 22.13 m standard plots with an average slope of 9$\%$. RUSLE3D was designed to account for more complex, 3D topography with converging and diverging flows. In RUSLE3D the topographic potential for erosion at any given point is represented by a 3D topographic factor LS_{3D}, which is a function of the upslope contributing area and the angle of the slope.

In this spatially and temporally distributed model RUSLE3D is modified by the use of a event-based [..[130]]R-factor derived from rainfall intensity at each time step. For each time step this model computes the parameters for RUSLE3D – an event-based erosivity factor, the slope of the topography, the flow accumulation, and the 3D topographic factor – and then solves

---

[118] removed: sum of the second order derivatives of elevation (?):

[119] removed: where:

[120] removed: ε_g is the gravitational diffusion coefficient

[121] removed: $\mathrm{m}^2\ \mathrm{s}^{-1}$

[122] removed: ∇ is the topographic divergence

[123] removed: m^{-1}

[124] removed: .

[125] removed: universal soil loss equation 3D model

[126] removed: The Revised Universal Soil Loss Equation for Complex Terrain (

[127] removed:)

[128] removed: equation

[129] removed: As an empirical equation the predicted soil loss is spatially and temporally averaged.

[130] removed: r-factor derived from the

the RUSLE3D equation for [..[131]]the rate of soil loss (i.e. the net soil erosion rate). The soil erosion rate is then used to simulate landscape evolution in a detachment capacity limited soil erosion regime.

2.3.1 [..[132]]Erosivity factor

The erosivity factor R in USLE and RUSLE is the combination of the total energy and peak intensity of a rainfall event, representing the interaction between the detachment of sediment particles and the transport capacity of the flow. It can be calculated as the product of the the kinetic energy of the rainfall event E and its maximum 30 min intensity I_{30} [..[133]](Brown and Foster, 1987; Renard et al., 1997; Panagos et al., 2015, 2017). In this model, however, the erosivity factor is derived at each time step as a function of kinetic energy, rainfall [..[134]]depth, rainfall intensity, and time. First rain energy is derived from rainfall intensity [..[135]][..[136]] (Brown and Foster, 1987; Yin et al., 2017):

$$\frac{\mathsf{e_r}}{\mathsf{e_0}} = 1. - \mathsf{b}\,\exp\left(\frac{\mathsf{i_r}}{\mathsf{i_0}}\right) \tag{20}$$

where:

$e_r$is unit rain energy $[\mathrm{MJ\,ha^{-1}\;mm^{-}1}]$

i_r is rainfall intensity $[\mathrm{mm\,h^{-1}}]$[..[137]]

b is empirical coeficient

i_0 is reference rainfall intensity $[\mathrm{mm\,h^{-1}}]$

e_0 is reference energy $[\mathrm{MJ\,ha^{-1}\;mm^{-}1}]$.

The parameters for this equation were derived from observed data published for different regions by Panagos et al. (2017). Then the event-based erosivity index R_e is calculated as the product of unit rain energy, rainfall [..[138]]depth, rainfall intensity, and time: [..[139]]

$$\mathsf{R_e} = \mathsf{e_r}\;\mathsf{v_r}\;\mathsf{i_r}\;\Delta \mathsf{t} \tag{21}$$

---

[131] removed: sediment flow. The sediment flow is

[132] removed: Event-based erosivity

[133] removed: (Brown and Foster, 1987; Renard et al., 1997)

[134] removed: volume

[135] removed: (Brown and Foster, 1987):

[136] removed:

$$e_r = 0.29\;(1. - 0.72\;exp(-0.05\;i_r))$$

[137] removed: .

[138] removed: volume

[139] removed:

$$R_e = e_r\;v_r\;i_r\;t_r$$

where:

R_e is the event-based erosivity index $[\mathrm{MJ\,mm\,ha^{-1}\,hr^{-1}}]$

v_r is the rainfall [..[140]]depth [mm] derived from [..[141]]$v_r = i_r\ \Delta t$

[..[142]]Δt is the change in time [s].

2.3.2 Flow accumulation

The upslope contributing area per unit width a is determined by flow accumulation [..[143]](the number of grid cells draining into a given grid cell) multiplied by grid cell width (Fig. 3d). Flow accumulation is calculated using a multiple flow direction algorithm (Metz et al., 2009) based on A^T least cost path searches (Ehlschlaeger, 1989). The multiple flow direction algorithm implemented in GRASS GIS as the module r.watershed is computationally efficient, does not require sink filling, and can navigate nested depressions and other obstacles.

2.3.3 3D topographic factor

The 3D topographic factor [..[144]]LS_{3D} is calculated as a function of the [..[145]]upslope contributing area [..[146]]and the slope (Fig. 3e). [..[147]][..[148]]

$$LS_{3D} = (m+1)\left(\frac{a}{a_0}\right)^{m}\left(\frac{\sin\beta}{\beta_0}\right)^{n} \tag{22}$$

where:

LS_{3D} is the dimensionless topographic [..[149]]factor

a is upslope contributing area per unit width [m]

a_0 is the length of the standard USLE plot [22.1 m]

β is the angle of the slope [°]

m is an empirical coefficient

n is an empirical coefficient

β_0 is the slope of the standard USLE plot [0.09°].

---

[140] removed: volume

[141] removed: $v_r = i_r\ t_r$

[142] removed: t_r is the time interval

[143] removed: times

[144] removed: $LS_{3D}(x, y)$

[145] removed: flow accumulation, representing the

[146] removed: ,

[147] removed: The empirical coefficients m and n for the upslope contributing area and the slope can range from 0.2 to 0.6 and 1.0 to 1.3 respectively with low values representing dominant sheet flow and high values representing dominant rill flow.

[148] removed:

$$LS_{3D} = (m+1.0)\ (a(x,y)\ a_0^{-1})^m\ (sin(\beta)\ \beta_0^{-1})^n$$

[149] removed: (length-slope)

The empirical coefficients m and n for the upslope contributing area and the slope can range from 0.2 to 0.6 and 1.0 to 1.3 respectively with low values representing dominant sheet flow and high values representing dominant rill flow.

2.3.4 [..[150]]Detachment limited erosion rate

[..[151]]The erosion rate is a function of the event-based erosivity factor, [..[152]]soil erodibility factor, [..[153]]3D topographic factor, [..[154]]landcover factor, and [..[155]]prevention measures factor (Fig. 3[..[156]]d):

$$E = R_e \; K \; LS_{3D} \; C \; P \tag{23}$$

where:

E is [..[157]]soil erosion rate (soil loss) $[\mathrm{kg\,m^{-2}\,min^{-1}}]$

R_e is the event-based erosivity factor $[\mathrm{MJ\,mm\,ha^{-1}\,hr^{-1}}]$

K is the soil erodibility factor $[\mathrm{ton\,ha\,hr\,ha^{-1}\,MJ^{-1}\,mm^{-1}}]$

LS_{3D} is the dimensionless topographic (length-slope) factor

C is the dimensionless [..[158]]landcover factor

P is the dimensionless prevention measures factor.

[..[159]]The detachment limited erosion represented by RUSLE3D leads to the simulated change in elevation[..[160]]:

$$\Delta z_s = D_c \rho_s^{-1} = E \; \rho_s^{-1} \tag{24}$$

which is combined with Eq. (3) for gravitational diffusion.

2.4 Unit [..[161]]Streampower Erosion Deposition (USPED)

[..[162]]USPED estimates net erosion-deposition as the divergence of sediment flow in transport capacity limited soil erosion [..[163]]regime. The amount of soil detached is close to the amount of sediment that water flow can carry. As a transport

---

[150] removed: Sediment flow

[151] removed: Sediment flow

[152] removed: the

[153] removed: the

[154] removed: cover

[155] removed: the

[156] removed: f

[157] removed: sediment flow

[158] removed: land cover

[159] removed: For

[160] removed: Δz is derived from equation **??** for landscape evolution in an detachment limited soil erosion regime and then equation 3for the settling of sediment particles due to

[161] removed: streampower erosion deposition model

[162] removed: The Unit Stream Power Erosion Deposition (USPED) model

[163] removed: regimes. At transport capacity shallow flows of water are carrying as much sediment possible – more sediment is being detached than can be transported

capacity limited model USPED predicts erosion where transport capacity increases and deposition where transport capacity decreases. The influence of topography on [..[164]]sediment flow is represented by a topographic sediment transport factor, while the influence of soil and landcover are represented by factors adopted from USLE and RUSLE (Mitasova et al., 1996). [..[165]]Sediment flow is estimated by computing the event-based erosivity factor (R_e) using Eq. 21, the slope and aspect of the topography, the flow accumulation with a multiple flow direction algorithm, the topographic sediment transport factor, [..[166]]and sediment flow at transport capacity[..[167]]. Net erosion-deposition is then computed as the divergence of [..[168]]sediment flow.

2.4.1 Topographic sediment transport factor

[..[169]]Using the unit stream power concept presented by Moore and Burch (1986), the 3D topographic factor (Eq. 22) for RUSLE3D is [..[170]]modified to represent the topographic sediment transport factor ([..[171]]LS_T) – the topographic component of overland flow at sediment transport capacity: [..[172]]

$$\mathsf{LS_T} = \mathsf{a}^{\mathsf{m}}\ (\sin\beta)^{\mathsf{n}} \tag{25}$$

where:

[..[173]]LS_T is the topographic sediment transport factor

a is the upslope contributing area per unit width [[..[174]]m]

β is the angle of the slope [°]

m is an empirical coefficient

n is an empirical coefficient.

---

[164] removed: erosion and deposition in USPED

[165] removed: Net erosion-deposition

[166] removed: the

[167] removed: , and

[168] removed: the

[169] removed: The

[170] removed: adapted

[171] removed: LST

[172] removed:

$$LST = a^m\ (\sin\beta)^n$$

[173] removed: LST

[174] removed: m

2.4.2 Transport limited sediment flow and net erosion-deposition

[..[175]]Sediment flow at transport capacity is a function of the event-based rainfall factor, [..[176]]soil erodibility factor, [..[177]]topographic component of overland flow, [..[178]]landcover factor, and [..[179]]prevention measures factor:

$$T = R_e\ K\ C\ P\ LST$$

[..[180]]

[..[181]][[..[182]]]

[..[183]][[..[184]]]

[..[185]][[..[186]]]

[..[187]]

[..[188]]

$$T = R_e\ K\ C\ P\ LS_T \tag{26}$$

where:

T is sediment flow at transport capacity $[\mathrm{kg\,m^{-1}\ s^{-1}}]$

R_e is the event-based rainfall factor $[\mathrm{MJ\,mm\,ha^{-1}\ hr^{-1}}]$

K is the soil erodibility factor $[\mathrm{ton\,ha\,hr\,ha^{-1}\ MJ^{-1}\ mm^{-1}}]$

C is the dimensionless land cover factor

P is the dimensionless prevention measures factor.

Net erosion-deposition [..[189]]is estimated as the divergence of sediment flow, assuming that sediment flow is equal to sediment transport capacity:

$$d_s = \frac{\partial(T\ \cos\alpha)}{\partial x} + \frac{\partial(T\ \sin\alpha)}{\partial y}$$

---

[175] removed: The sediment

[176] removed: the

[177] removed: the

[178] removed: the

[179] removed: the

[180] removed: where:

[181] removed: T is sediment flow at transport capacity

[182] removed: $\mathrm{kg\,m^{-1}\ s^{-1}}$

[183] removed: R_e is the event-based rainfall factor

[184] removed: $\mathrm{MJ\,mm\,ha^{-1}\ hr^{-1}}$

[185] removed: K is the soil erodibility factor

[186] removed: $\mathrm{ton\,ha\,hr\,ha^{-1}\ MJ^{-1}\ mm^{-1}}$

[187] removed: C is the dimensionless land cover factor

[188] removed: P is the dimensionless prevention measures factor.

[189] removed: at transport capacity

[..[190]]

[..[191]][[..[192]]]

[..[193]][[..[194]]][..[195]]

$$d_s = \frac{\partial(T\ \cos\alpha)}{\partial x} + \frac{\partial(T\ \sin\alpha)}{\partial y} \tag{27}$$

where:

d_s is net erosion-deposition $[\mathrm{kg\,m^{-2}\,s^{-1}}]$

α is the aspect of the topography (i.e. the direction of flow) $[°]$.

With USPED the simulated change in elevation [..[196]]$\Delta z_s = d_s$ is derived from equation 2 for landscape evolution and then equation 3 for [..[197]]gravitational diffusion.

3 Case study

Military activity is a high-impact land use that can cause significant physical alteration to the landscape. Erosion is a major concern for military installations, particularly at training bases, where the land surface is disturbed by off-road vehicles, foot traffic, and munitions. Off-road vehicles and foot traffic by soldiers cause the loss of vegetative cover, the disruption of soil structure, soil compaction, and increased runoff due to reduced soil capacity for water infiltration (Webb and Wilshire, 1983; McDonald, 2004). Gullies – ephemeral channels with steep headwalls that incise into unconsolidated soil to depths of meters – are a manifestation of erosion common to military training installations like Ft. Bragg in North Carolina and the [..[198]]Piñon Canyon Maneuver Site in Colorado. While the local development of gullies can restrict the maneuverability of troops and vehicles during training exercises, pervasive gullying across a landscape can degrade an entire training area (Huang and Niemann, 2014).

To test the effectiveness of the different models in r.sim.terrain we compared the simulated evolution of a highly eroded subwatershed of Patterson Branch [..[199]]on Fort Bragg, North Carolina against a timeseries of airborne lidar surveys. The models – SIMWE, RUSLE3D, and USPED – were tested in steady state and dynamic modes for [..[200]]design storms with constant rainfall.

---

[190] removed: where:

[191] removed: d_s is net erosion-deposition

[192] removed: $\mathrm{kg\,m^{-2}\,s^{-1}}$

[193] removed: α is the aspect of the topography

[194] removed: $\circ$

[195] removed: .

[196] removed: Δz

[197] removed: the settling of sediment particles due to

[198] removed: Piñon

[199] removed: Creek

[200] removed: constant rainfall, design storms , and recorded

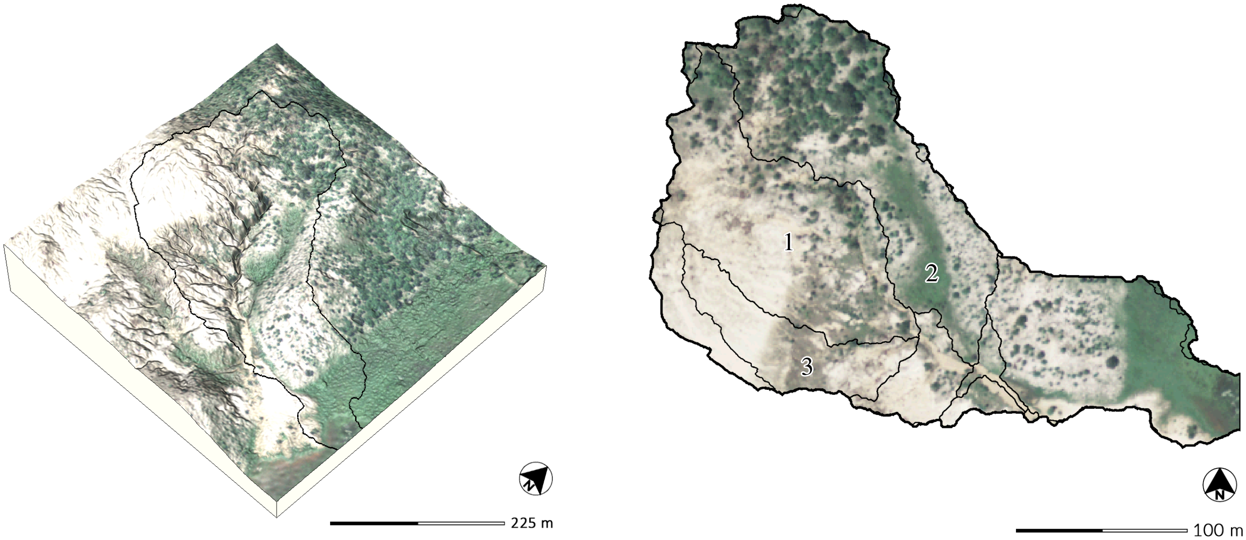

a.

b.

Figure 4. Subwatershed with 2014 orthoimagery (a) draped over the 2016 digital elevation model and (b) drainage areas with 2014 orthoimagery, Patterson Branch[..[202]], Fort Bragg, NC, USA

3.1 Patterson Branch[..[201]]

With 650 km^2 of land Fort Bragg is the largest military installation in the US and has extensive areas of bare, erodible soils on impact areas, firing ranges, landing zones, and dropzones. It is located in the Sandhills region of North Carolina with a Longleaf Pine and Wiregrass Ecosystem (Sorrie et al., 2006). The study landscape – a subwatershed of Patterson Branch [..[203]](Figure 4) in the Coleman Impact Area – is pitted with impact craters from artillery and mortar shells and has an active, approximately 2 m deep gully. It is a Pine-Scrub Oak Sandhill community composed primarily of Longleaf Pine ([..[204]]*Pinus palustris*) and Wiregrass ([..[205]]*Aristida stricta*) on Blaney and Gilead loamy sands (Sorrie, 2004). Throughout the Coleman Impact Area frequent fires ignited by live munitions drive the ecological disturbance regime of this fire adapted ecosystem. In 2016 the 450 m^2 study site was 43.24% bare ground with predominately loamy sands, 39.54% covered by the Wiregrass community, and 17.22% forested with the Longleaf Pine community (Figure 5[..[206]]a). We hypothesize that the elimination of forest cover in the impact zone triggered extensive channelized overland flow, gully formation, and sediment transport into the creek.

---

[201] removed: Creek

[203] removed: Creek

[204] removed: Pinus palustris

[205] removed: Aristida stricta

[206] removed: c

Timeseries of digital elevations models and landcover maps for the study landscape were generated from lidar pointclouds and orthophotography[..[207]]. The digital elevations models for 2004, 2012, and 2016 were interpolated at [..[208]]1 m resolution using the regularized spline with tension function (Mitasova and Mitas, 1993; Mitasova et al., 2005) from airborne lidar surveys collected by the NC Floodplain Mapping program and Fort Bragg. Unsupervised image classification was used to identify clusters of spectral reflectance in a timeseries of 1 m resolution orthoimagery collected by the National Agriculture Imagery Program. The landcover maps were derived [..[209]]from the classified lidar point clouds [..[210]]and the classified orthoimagery. Spatially variable soil erosion factors – the k-factor, c-factor, [..[211]]Manning's coefficient, and runoff [..[212]]rate – were then derived from the landcover and soil maps. The dataset for this study is hosted at https://github.com/baharmon/landscape_evolution_dataset under the ODC Open Database License (ODbL). The data is derived from publicly available data from the US Army, USGS, USDA, Wake County GIS, NC Floodplain Mapping Program, and the NC State Climate Office. There are detailed instructions for preparing the input data in the tutorial and a complete record of the commands used to process the sample data in the data log.

We used the geomorphons method of automated landform classification based on the openness of terrain (Jasiewicz and Stepinski, 2013) and the difference between the digital elevation models to analyze the changing morphology of the study area ([..[213]]Figures 5 & 6). The 2 m deep gully – its channels classified as valleys and its scour pits as depressions by geomorphons – has multiple mature branches and ends with a depositional fan. The gully has also developed depositional ridges beside the channels. Deep scour pits have developed where branches join the main channel and where the main channel has sharp bends. A new branch has begun to form in a knickzone classified as a mix of valleys and hollows on a grassy swale on the northeast side of the gully. Between 2012 and 2016 a depositional ridge [..[214]]developed at the foot of this nascent branch where it would meet the main channel. The 2016 minus 2012 DEM of Difference (DoD) – i.e. the difference in elevation [..[215]](Figures 5c & 6c) – shows a deepening of the main channel by approximately 0.2 m and [..[216]]scours pits by approximately 1 m, while depositional ridges have formed and grown up to approximately 1 m [..[217]]high. The DoD also shows that 244.60 m^3 of sediment were deposited on the depositional fan between 2012 and 2016.

---

[207] removed: (Figure 5a-c).
[208] removed: 0.3
[209] removed: by fusing
[210] removed: with
[211] removed: mannings
[212] removed: rates
[213] removed: Figure 5 d-f
[214] removed: has
[215] removed: between 2012 and 2016 (Figure 5d)
[216] removed: the
[217] removed: or more.

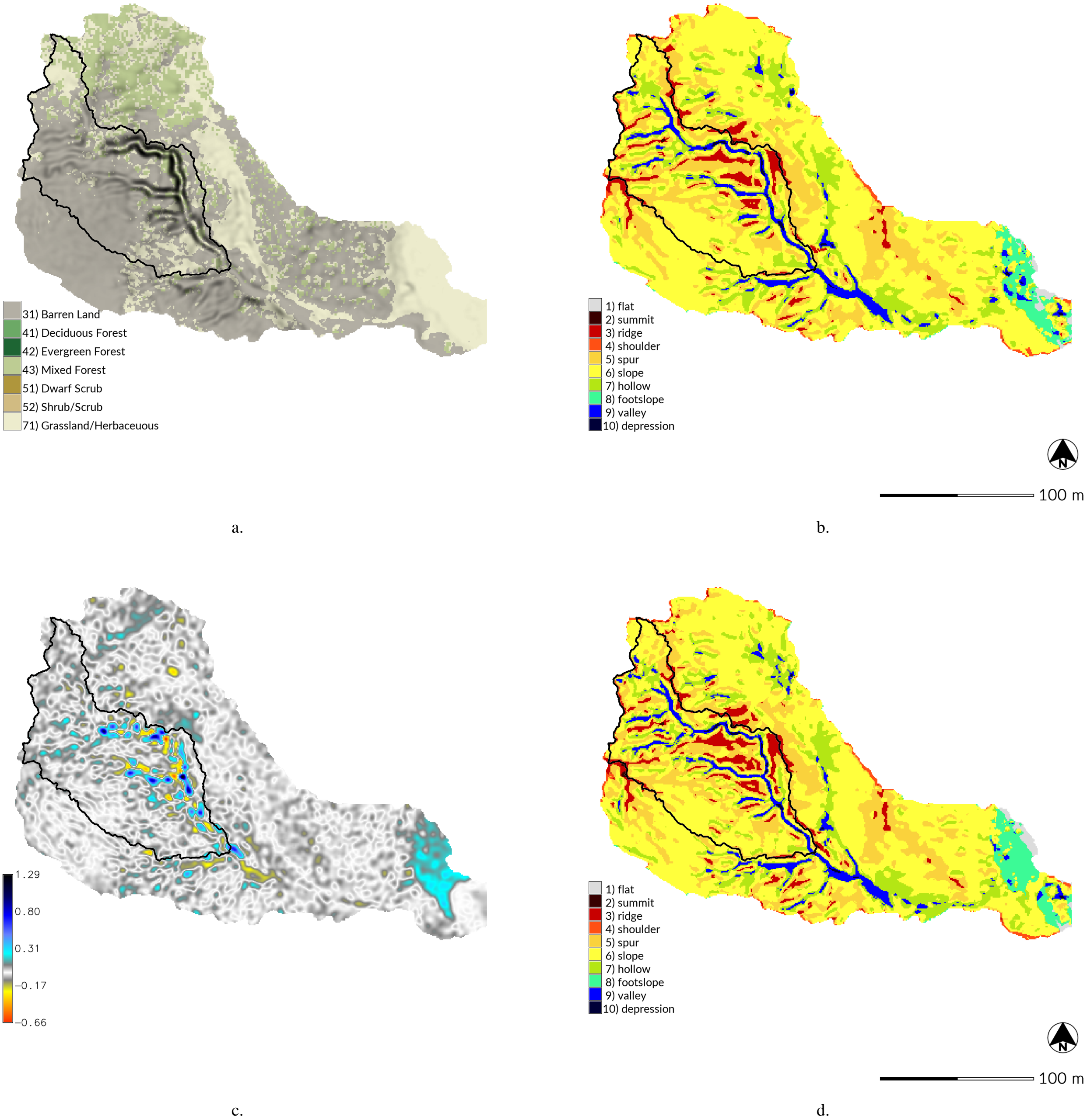

Figure 5. Morphological Change, Study Subwatershed, Patterson Branch[..218], Fort Bragg, NC, USA. (a) Landcover in 2014, (b) landforms in 2012, (c) elevation difference between 2012-2016 [m], and (d) landforms in 2016.

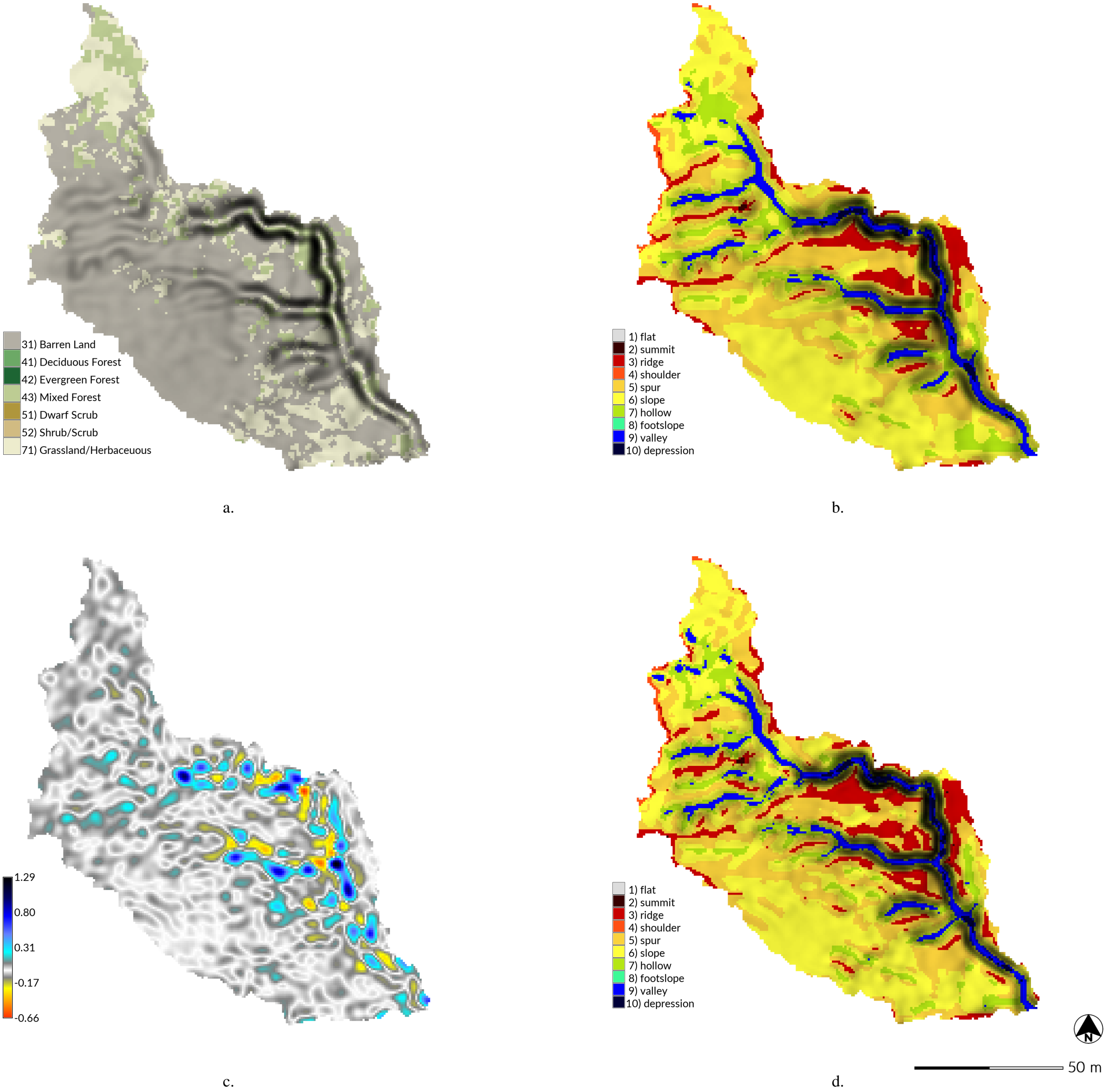

a. b.

c. d.

Figure 6. Detailed Morphological Change, Drainage Area 1, Study Subwatershed, Patterson Branch, Fort Bragg, NC, USA. (a) Land-cover in 2014, (b) landforms in 2012, (c) elevation difference between 2012-2016 [m], and (d) landforms in 2016.

3.2 Simulations

We ran a sequence of r.sim.terrain simulations with design storms for the Patterson Branch [..219]subwatershed study area to [..220]demonstrate the capabilities of the RUSLE3D, [..221]USPED, and SIMWE models (Table 2). [..222]To analyze the results of the simulations, we compared net differences in elevation morphological features, and volumetric change. While r.sim.terrain can use rainfall records, we used design storms to demonstrate and test the basic capabilities of the model. Our design storms were based off the peak rainfall values in records from the State Climate Office of North Carolina. We used RUSLE3D to simulate landscape evolution in a dynamic, detachment capacity limited soil erosion regime for a $120\,\mathrm{min}$ [..223]design storm with 3 min intervals and a constant rainfall intensity of $50\,\mathrm{mm\,hr^{-1}}$ [..224](Figure [..225]7). [..226][..227][..228]We used USPED to simulate landscape evolution in a dynamic, transport capacity limited soil erosion [..229]regime for a 120 min design storm with 3 min intervals and a constant rainfall intensity of 50 $\mathrm{mm\,hr^{-1}}$ (Figure [..230]8). [..231]We used SIMWE to simulate landscape evolution in a steady state, variable erosion-deposition soil erosion regime for a $120\,\mathrm{min}$ [..232]design storm with a constant rainfall intensity of $50\,\mathrm{mm\,hr^{-1}}$ [..233](Figure [..234]9). In all of the simulations a sink filling algorithm – an optional parameter in r.sim.terrain – was used to reduce the effects of positive feedback loops that cause the over-development of scour pits.

The simulations were automated and run in parallel using Python scripts that are available in the software repository. The simulations can be reproduced using these scripts and the study area dataset by following the instructions in the Open Science Framework repository at https://osf.io/tf6yb/. The simulations were run in GRASS GIS 7.4 on a desktop computer with 64-bit Ubuntu 16.04.4 LTS, 8 x 4.20 GHz Intel Core i7 7700K CPUs, and 32 GB RAM. Simulations using SIMWE are far more computationally intensive than RULSE3D or USPED, but support multi-threading when compiled with OpenMP. Dynamic simulations of RUSLE3D and USPED [..235]took 2 min 36 s and 3 min 14 s respectively to run on a single thread, while [..236]the steady state simulation for SIMWE took 44 min [..237]51 s running on 6 threads (Table 2).

---

[219] removed: Creek

[220] removed: test dynamic and steady state flow regimes in the SIMWE,

[221] removed: and USPED

[222] removed: RUSLE3D was used to simulate

[223] removed: events with rainfall intensities

[224] removed: for detachment capacity limited soil erosion regimes for both dynamic and steady state flow regimes using RUSLE3D

[225] removed: **??**a-c

[226] removed: USPED was used to simulate 120

[227] removed: events with rainfall intensities of

[228] removed: $^{-1}$ for

[229] removed: regimes for both dynamic and steady state flow regimes

[230] removed: **??**d-f

[231] removed: SIMWE was used to simulate

[232] removed: events with rainfall intensities

[233] removed: for erosion-deposition and detachment limited soil erosion regimes in steady state flow regimes

[234] removed: **??**

[235] removed: each took

[236] removed: steady state simulations for SIMWE each took 84

[237] removed: 13

Table 2. Landscape evolution simulations

Flow regime	Model	Intensity	Duration	Interval	m	n	ρ_s	Threads	Runtime
Dynamic	RUSLE3D	50 mm hr^{-1}	120 min	3 min	0.4	1.3			2 min 36 s
Dynamic	USPED	50 mm hr^{-1}	120 min	3 min	1.5	1.2	1.6		3 min 14 s
Steady state	SIMWE	50 mm hr^{-1}	120 min	120 min			1.6	6	44 min 51 s

Table 3. Volumetric change

Difference of DEMs (DoD)	Threshold [m]	Erosion [m^3]	Deposition [m^3]	Net change [m^3]
2016 - 2012	±0.18	152.96	807.74	654.77
Simulated with RUSLE3D - 2012	None	1480.75	0	-1480.75
Simulated with USPED - 2012	None	1235.08	727.46	-507.62
Simulated with SIMWE -2012	None	758.56	608.91	-149.66

3.3 Results

We used the Difference in DEMs to compute volumetric changes between the lidar surveys and the simulations (Table 3). We applied a threshold of ±0.18 m to the lidar surveys since they had a vertical accuracy at a 95% confidence level of 18.15 cm based on a 9.25 cm root mean square error (RMSEz) for non vegetated areas in accordance with the National Digital Elevation Program guidelines (North Carolina Risk Management Office, 2018). Given the presence of the mature gully with ridges along its banks, we hypothesize that the study landscape had previously been dominated by a detachment limited soil erosion regime, but – given the net change of 654.77 m^3 – had switched to a transport capacity limited or variable erosion-deposition regime during our study period.

The dynamic RUSLE3D [..[238]]simulation carved a deep incision in the [..[239]]main gully channel where water accumulated (Figure [..[240]]7). As a detachment capacity limited model RUSLE3D's results were dominated by erosion and thus negative elevation change. [..[241]]It eroded 1480.75 m^3 of sediment with no deposition.

The dynamic USPED simulation eroded the banks of the gully and deposited in channels causing the gully grow wider and shallower (Figure [..[242]]8). As a transport capacity limited model USPED generated a distributed pattern with both erosion and deposition[..[243]]. Erosion far exceeded deposition with 1235.08 m^3 of sediment eroded and 727.46 m^3 deposited for

---

[238] removed: simulation deepened the main channel of

[239] removed: gully, while the dynamic USPED simulation eroded the banks of the gully and deposited in channels causing the gully grow wider and shallower

[240] removed: **??**).

[241] removed: RUSLE3D carved a deep incision in the main gully channel where water and sediment flow accumulated

[242] removed: **??**c).

[243] removed: and thus negative and positive elevation change .

a net change of -507.62 m^3. While USPED's pattern of elevation change was grainy and fragmented, it captured the process of channel filling and widening expected with a transport capacity limited soil erosion regime[..[244]].

The steady state SIMWE [..[245]]simulation for a variable erosion-deposition [..[246]]regime predicted the morphological processes and features expected of its regime including gradual aggradation, channel widening, the formation of depositional ridges along the thalweg of the channel[..[247]], and the development of the depositional fan (Figure [..[248]]9). SIMWE was the closest to the observed baseline volumetric change. It balanced erosion and deposition with 785.56 m^3 of sediment eroded and 608.91 m^3 deposited for a net change of -149.66 m^3. Only the SIMWE simulation deposited sediment on the depositional fan. While the difference of lidar surveys showed that 244.60 m^3 of sediment were deposited on the fan, SIMWE predicted that 54.05 m^3 would be deposited.

[..[249]]

[..[250]]SIMWE was unique in simulating unsteady flows (Figure 9a) and fine-scale geomorphological processes such as the development of depositional ridges and a depositional fan. While USPED generated a grainy pattern of erosion and deposition, it was much faster than SIMWE (Table 2) and still simulated the key morphological patterns and processes – channel incision, filling, and widening. Given their speed and approximate modeling of erosive processes, RUSLE3D and USPED are effective for simulating landscape evolution [..[251]][..[252]]on large rasters. RUSLE3D for example has been used to model erosion for the entire 650 km^2 Fort Bragg installation at 9 m resolution (Levine et al., 2018).

4 Discussion

Limitations of this landscape evolution model include shallow overland flow, units, computation time, and raster size. r.sim.terrain only models shallow overland flows, not fluvial processes or subsurface flows. It requires data – including elevation and rainfall intensity – in metric units. The implementation of SIMWE in GRASS GIS is computationally intensive and may require long computation times even with multithreading. Because SIMWE uses a Green's function Monte Carlo

---

[244] removed: (Figure **??**f)

[245] removed: simulations predicted more realistic patterns of landscape evolution (Figure **??**). For transport limited and

[246] removed: regimes SIMWE simulated channel wideningand

[247] removed: (Figure **??**c). For a detachment limited soil erosion regime SIMWE simulated major erosion driving the continued development of the gully network including the spread of rills and the evolution of the nascent branch into a full fledged channel

[248] removed: **??**f). The detachment limited simulation also formed extensive ridges beside the gully channels (Figure **??**f), continuing the development of channel-side ridges observed in the 2012 and 2016 landform maps (Figure 5e-f).

[249] removed: Given the presence of an active gully with ridges along its banks, this landscape is dominated by a detachment limited soil erosion regime. The detachment limited SIMWE simulation generated the morphological features – the deeply incised gully channels, scour pits, and ridges along the channels – characteristic of its erosion regime, realistically simulating landscape evolution at the scale of a subwatershed. The erosion-deposition and transport limited SIMWE simulations also generated the morphological processes and features that would be expected in these regimes – gradual aggradation and the formation of a depositional ridge along the thalweg of the channel.

[250] removed: While RUSLE3D and USPED produced less realistic patterns of landscape evolution than SIMWE, these models were much faster and still generated

[251] removed: at regional scales, i.e. for landscapes greater than 10

[252] removed: ^{2}.

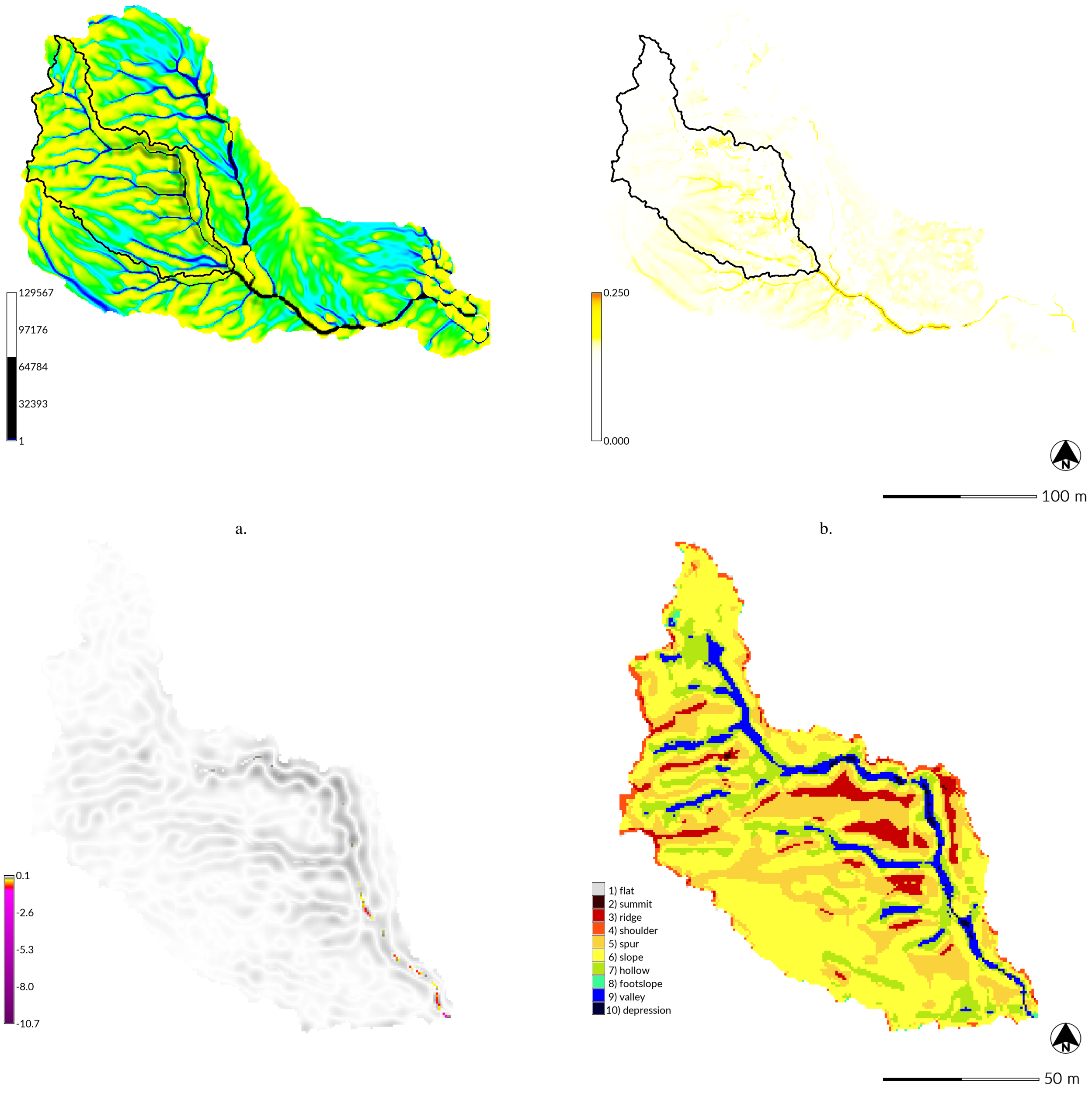

a.

b.

c.

d.

Figure 7. Dynamic simulation with RUSLE3D for a 120 min event with a rainfall intensity of 50 $\mathrm{mm\,hr^{-1}}$ at 1 m resolution for the Study Subwatershed (a-b) and Drainage Area 1 (c-d) on Patterson Branch, Fort Bragg, NC. The (a) flow accumulation and (b) erosion $[\mathrm{kg\,m^{-2}\,s^{-1}}]$ for the Study Subwatershed in the final 3 min timestep. The (c) net difference $[\mathrm{m}]$ and (d) landforms for Drainage Area 1.

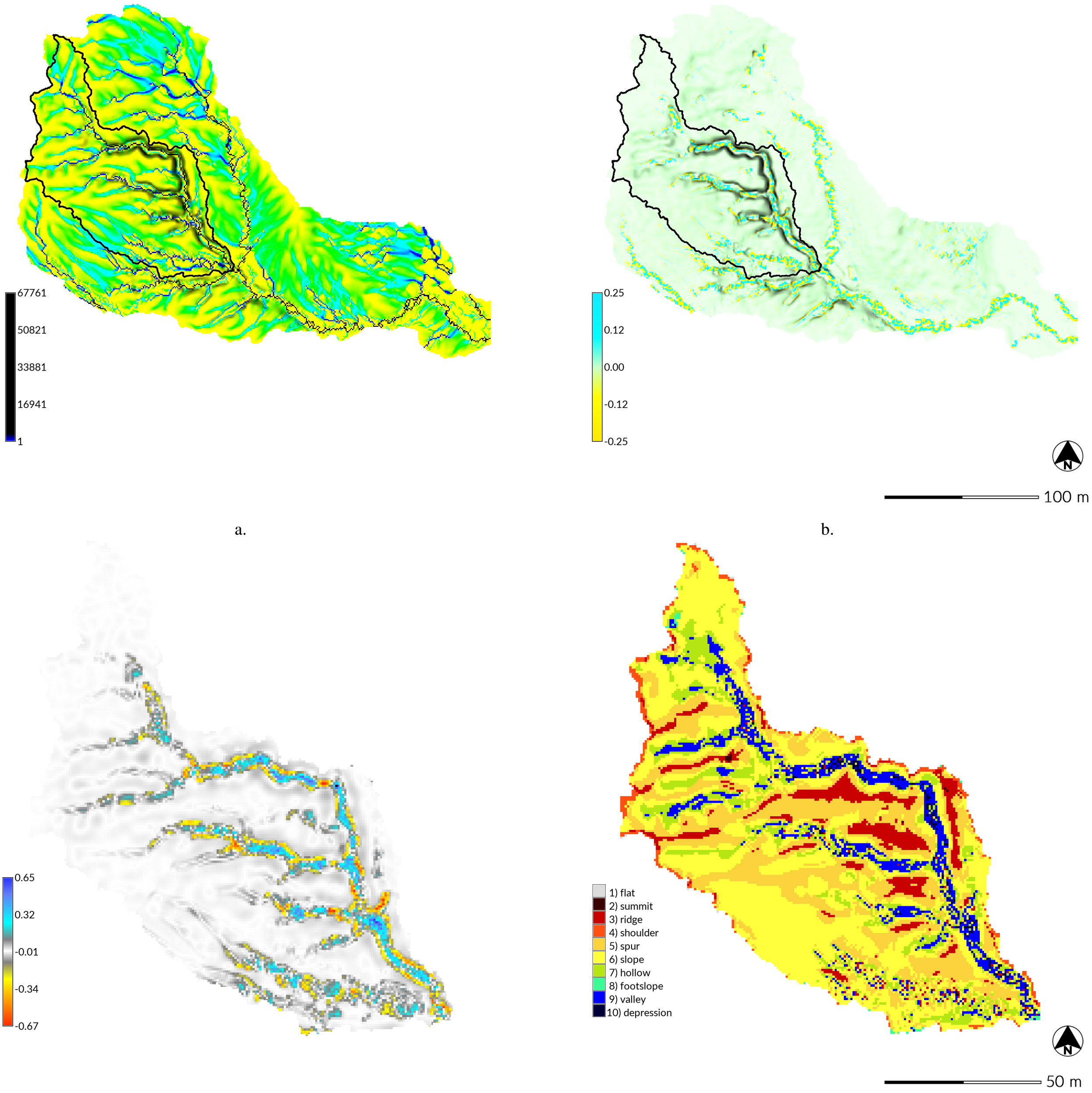

a.

b.

c.

d.

Figure 8. Dynamic [..[253]]simulation with USPED [..[254]]for a 120 min event with a rainfall intensity of $50\,\mathrm{mm\,hr^{-1}}$ at 1 m resolution for the Study Subwatershed (a-b) and Drainage Area 1 (c-d) on Patterson Branch, Fort Bragg, NC. The (a) flow accumulation and (b) erosion-deposition $[\mathrm{kg\,m^{-2}\,s^{-1}}]$ for the Study Subwatershed in the final 3 min timestep. The (c) net difference [m] and (d) landforms for Drainage Area 1.

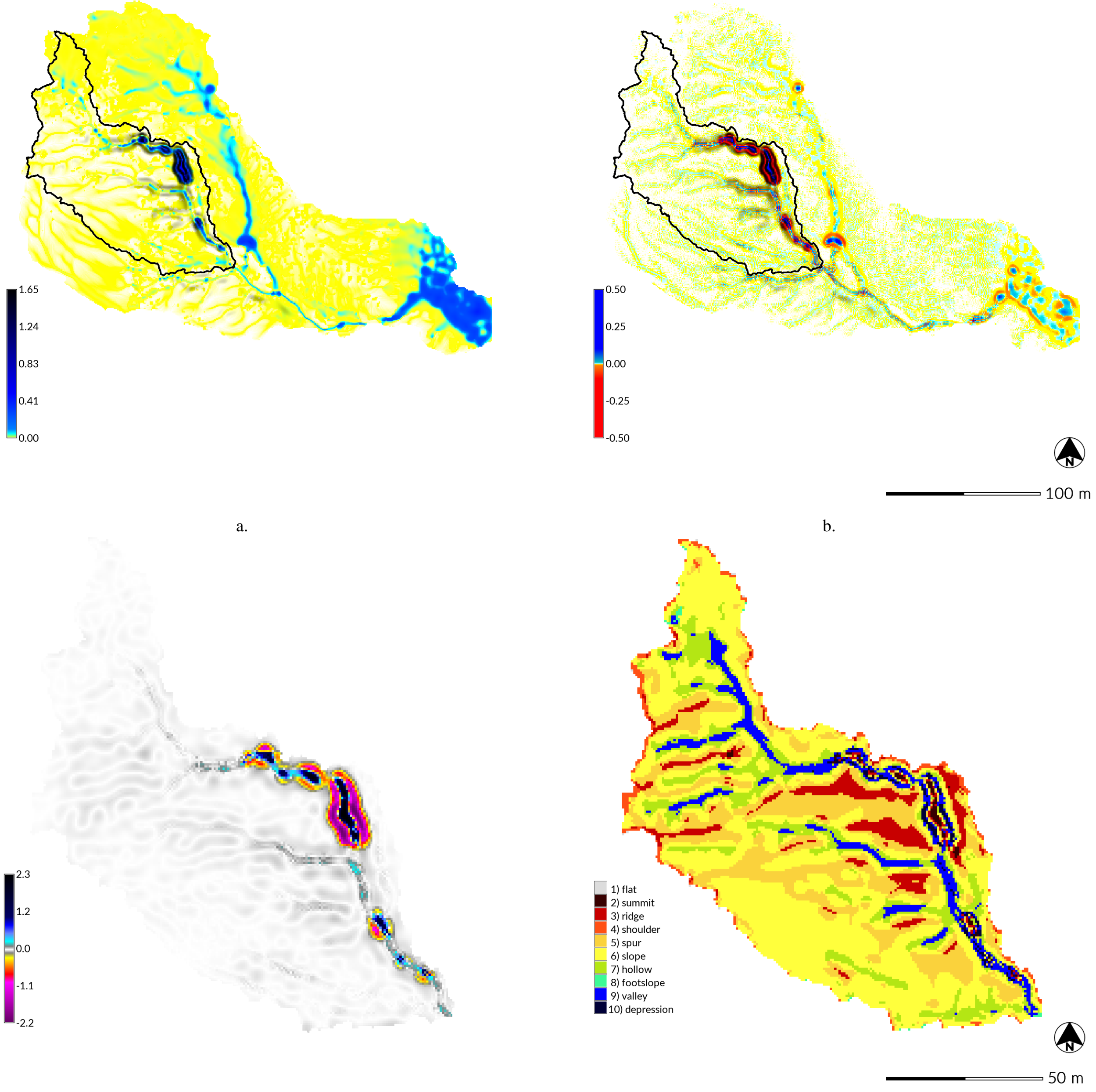

a. b. c. d.

Figure 9. Steady state SIMWE simulations for a $120\ \mathrm{min}$ [..255]event with a rainfall [..256]intensity of $50\ \mathrm{mm\,hr^{-1}}$ at $1\ \mathrm{m}$ resolution for the Study Subwatershed (a-b) and [..257]Drainage Area 1 (c-d) on Patterson Branch, Fort Bragg, NC. The (a) depth of unsteady flow $[\mathrm{m}]$ and (b) erosion-deposition $[\mathrm{kg\,m^{-2}\ s^{-1}}]$ for the Study Subwatershed. The (c) net difference $[\mathrm{m}]$ and (d) landforms for Drainage Area 1.

solution of the sediment transport equation, the accuracy, detail, and smoothness of the results depend on the number of random walkers. While a large number of random walkers will reduce the numerical error in the path sampling solution, it will also greatly increase computation time. A customized compilation of GRASS GIS is needed to run SIMWE with more than 7 million random walkers. This limits the size of rasters that can be easily processed with SIMWE, while RUSLE3D and USPED are much faster, computationally efficient, and can easily be run on much larger rasters.

In the future we plan to assess this model by comparing simulations against a monthly timeseries of submeter resolution surveys by unmanned aerial systems and terrestrial lidar. We also plan to develop a case study demonstrating how the model can be used as a planning tool for landscape restoration. Planned enhancements to the model include modeling subsurface flows, accounting for bedrock, and a reverse landscape evolution mode for backward modeling.

5 Conclusions

The short-term landscape evolution model r.sim.terrain can [..[258]]simulate the development of gullies, rills, and hillslopes by overland water erosion for a range of hydrologic and soil erosion regimes. The model is novel for simulating landscape evolution based on unsteady flows. The landscape evolution model was tested with a series of simulations for different hydrologic and soil erosion regimes for a highly eroded sub-watershed on Fort Bragg with an active gully. For each regime it generated the morphological processes and features expected. The physics-based SIMWE model [..[259]]simulated morphological processes [..[260]]for a variable erosion-deposition [..[261]]regime such as gradual aggradation, channel widening, scouring, the development of depositional ridges along the thalweg, and the growth of the depositional fan. The empirical RUSLE3D [..[262]]model simulated channel incision in a detachment limited soil erosion [..[263]]regime, while the semi-empirical USPED model simulated channel widening and filling [..[264]]in a transport limited regime. Since r.sim.terrain is a GIS-based model that [..[265]]simulates fine-scale morphological processes and features, [..[266]]it can easily and effectively be used in conjunction with other GIS-based tools for geomorphological research, land management and conservation, erosion control, and landscape restoration.

Code and data availability. As a work of open science this study is reproducible, repeatable, and recomputable. Since the data, model, GIS, dependencies are all free and open source, the study can easily be reproduced. The landscape evolution model has been implemented

---

[258] removed: realistically

[259] removed: realistically simulated short-term topographic change for steady state hydrologic regimes at sub-watershed to watershed scales. For detachment limited soil erosion regimes it

[260] removed: including channel incision, channel widening, and the development of knickzones, rills, and scour pits. For transport limited and

[261] removed: regimes, it simulated processes such as channel aggradation, scouring, and

[262] removed: and USPED models approximated short-term topographic change at watershed to regional scales. For

[263] removed: regimes RUSLE3D simulated channel incision, while for transport limited regimes USPED

[264] removed: . Since it

[265] removed: realistically

[266] removed: r.sim.terrain

in Python as module for GRASS GIS, a free and open source GIS. The source code for the model is hosted on GitHub at https://github.com/baharmon/landscape_evolution under the GNU General Public License version 2. The code repository also includes Python scripts for running and reproducing the simulations in this paper. The digital object identifier (DOI) for the version of the software documented in this paper is: https://doi.org/10.5281/zenodo.2542921. There are detailed instructions for running this model in the manual at https://grass.osgeo.org/grass76/manuals/addons/r.sim.terrain.html and the tutorial at https://github.com/baharmon/landscape_evolution/blob/master/tutorial.md. The geospatial dataset for the study area is available on GitHub at https://github.com/baharmon/landscape_evolution_dataset under the Open Database License with the DOI: https://doi.org/10.5281/zenodo.2542929. The data log has a complete record of the commands used to process the sample data. The source code, scripts, data, and results are also hosted on the Open Science Framework at https://osf.io/tf6yb/ with the DOI: https://doi.org/10.17605/osf.io/tf6yb.

Author contributions. Brendan Harmon developed the models, code, data, case studies, and manuscript. Helena Mitasova contributed to the development of the models and case studies and revised the manuscript. Anna Petrasova and Vaclav Petras contributed to the development of the code. All authors read and approved the final manuscript.

Competing interests. The authors declare that they have no conflict of interest.

Acknowledgements. We acknowledge the GRASS GIS Development Community for developing and maintaining GRASS GIS.

References

Barton, C. M., Ullah, I., and Mitasova, H.: Computational Modeling and Neolithic Socioecological Dynamics: a Case Study from Southwest Asia, American Antiquity, 75, 364–386, http://www.jstor.org/stable/25766199, 2010.

Bechet, J., Duc, J., Loye, A., Jaboyedoff, M., Mathys, N., Malet, J. P., Klotz, S., Le Bouteiller, C., Rudaz, B., and Travelletti, J.: Detection of seasonal cycles of erosion processes in a black marl gully from a time series of high-resolution digital elevation models (DEMs), Earth Surface Dynamics, 4, 781–798, https://doi.org/10.5194/esurf-4-781-2016, 2016.

Braun, J. and Sambridge, M.: Modelling landscape evolution on geological time scales: a new method based on irregular spatial discretization, Basin Research, 9, 27–52, https://doi.org/10.1046/j.1365-2117.1997.00030.x, https://onlinelibrary.wiley.com/doi/abs/10.1046/j.1365-2117.1997.00030.x, 1997.

Brown, L. C. and Foster, G. R.: Storm Erosivity Using Idealized Intensity Distributions, Transactions of the American Society of Agricultural Engineers, 30, 0379 –0386, https://doi.org/http://dx.doi.org/10.13031/2013.31957, 1987.

Coulthard, T. J., Macklin, M. G., and Kirkby, M. J.: A cellular model of Holocene upland river basin and alluvial fan evolution, Earth Surface Processes and Landforms, 27, 269–288, https://doi.org/10.1002/esp.318, https://onlinelibrary.wiley.com/doi/abs/10.1002/esp.318, 2002.

Coulthard, T. J., Hancock, G. R., and Lowry, J. B. C.: Modelling soil erosion with a downscaled landscape evolution model, Earth Surface Processes and Landforms, 37, 1046–1055, https://doi.org/10.1002/esp.3226, https://onlinelibrary.wiley.com/doi/abs/10.1002/esp.3226, 2012.

Dabney, S., Vieira, D., Bingner, R., Yoder, D., and Altinakar, M.: Modeling Agricultural Sheet , Rill and Ephemeral Gully Erosion, in: ICHE 2014. Proceedings of the 11th International Conference on Hydroscience & Engineering, pp. 1119–1126, Karlsruhe, 2014.

Ehlschlaeger, C.: Using the A^T Search Algorithm to Develop Hydrologic Models from Digital Elevation Data, in: Proceedings of International Geographic Information Systems (IGIS) Symposium '89, pp. 275–281, Baltimore, MD, 1989.

Flanagan, D. C., Frankenberger, J. R., Cochrane, T. A., Renschler, C. S., and Elliot, W. J.: Geospatial Application of the Water Erosion Prediction Project (WEPP) Model, Transactions of the ASABE, 56, 591–601, https://doi.org/10.13031/2013.42681, https://www.fs.usda.gov/treesearch/pubs/43830, 2013.

Foster, G., Meyer, L., and Onstad, C.: An erosion equation derived from basic erosion principles, Transactions of the American Society of Agricultural Engineers, 20, 1977.

Goodwin, N. R., Armston, J., Stiller, I., and Muir, J.: Assessing the repeatability of terrestrial laser scanning for monitoring gully topography: A case study from Aratula, Queensland, Australia, Geomorphology, 262, 24 – 36, https://doi.org/https://doi.org/10.1016/j.geomorph.2016.03.007, http://www.sciencedirect.com/science/article/pii/S0169555X16300976, 2016.

GRASS Development Team: GRASS GIS, https://grass.osgeo.org.

Guertin, D. P., Goodrich, D. C., Burns, I. S., Korgaonkar, Y., Barlow, J., Sheppard, B. S., Unkrich, C., and Kepner, W.: Automated Geospatial Watershed Assessment Tool (AGWA), https://doi.org/10.1061/9780784479322.012, 2015.

Hobley, D. E., Adams, J. M., Siddhartha Nudurupati, S., Hutton, E. W., Gasparini, N. M., Istanbulluoglu, E., and Tucker, G. E.: Creative computing with Landlab: An open-source toolkit for building, coupling, and exploring two-dimensional numerical models of Earth-surface dynamics, Earth Surface Dynamics, 5, 21–46, https://doi.org/10.5194/esurf-5-21-2017, 2017.

Hofierka, J., Mitášová, H., and Neteler, M.: Geomorphometry in GRASS GIS, in: Geomorphometry, edited by Hengl, T. and Reuter, H. I., vol. 33 of *Developments in Soil Science*, pp. 387 – 410, Elsevier, https://doi.org/https://doi.org/10.1016/S0166-2481(08)00017-2, http://www.sciencedirect.com/science/article/pii/S0166248108000172, 2009.

Huang, X. and Niemann, J. D.: Simulating the impacts of small convective storms and channel transmission losses on gully evolution, in: Military Geosciences in the Twenty-First Century, edited by Harmon, R. S., Baker, S. E., and McDonald, E. V., Geological Society of America, https://doi.org/10.1007/978-1-4020-3105-2_18, 2014.

Jasiewicz, J. and Stepinski, T. F.: Geomorphons - a pattern recognition approach to classification and mapping of landforms, Geomorphology, 182, 147–156, https://doi.org/10.1016/j.geomorph.2012.11.005, 2013.

Jeziorska, J., Mitasova, H., Petrasova, A., Petras, V., Divakaran, D., and Zajkowski, T.: Overland Flow analysis using times series of sUAS-derived elevation models, in: ISPRS Annals of the Photogrammetry, Remote Sensing and Spatial Information Sciences, vol. 3, pp. 159–166, https://doi.org/10.5194/isprs-annals-III-8-159-2016, 2016.

Kasprak, A., Bransky, N. D., Sankey, J. B., Caster, J., and Sankey, T. T.: The effects of topographic surveying technique and data resolution on the detection and interpretation of geomorphic change, Geomorphology, 333, 1 – 15, https://doi.org/https://doi.org/10.1016/j.geomorph.2019.02.020, http://www.sciencedirect.com/science/article/pii/S0169555X19300546, 2019.

Koco, Š.: Simulation of gully erosion using the SIMWE model and GIS, Landsurface Analysis, 17, 81–86, 2011.

Levine, J., Wegmann, K., Mitasova, H., Eads, C., Lyons, N., Harmon, B., McCarther, C., Peart, S., Oberle, N., and Walter, M.: Freshwater Bivalve Survey for Endangered Species Branch Fort Bragg, NC, Tech. rep., North Carolina State University, Raleigh, NC, https://doi.org/10.13140/RG.2.2.17512.11521, 2018.

Malik, I.: Dating of small gully formation and establishing erosion rates in old gullies under forest by means of anatomical changes in exposed tree roots (Southern Poland), Geomorphology, 93, 421–436, https://doi.org/10.1016/j.geomorph.2007.03.007, 2008.

McDonald, K. W.: Military Foot Traffic Impact on Soil Compaction Properties, pp. 229–242, Springer Netherlands, Dordrecht, https://doi.org/10.1007/978-1-4020-3105-2_18, 2004.

Metz, M., Mitasova, H., and Harmon, R. S.: Fast Stream Extraction from Large , Radar- Based Elevation Models with Variable Level of Detail, pp. 237–242, 2009.

Mitas, L. and Mitasova, H.: Distributed soil erosion simulation for effective erosion prevention, Water Resources Research, 34, 505–516, https://doi.org/10.1029/97wr03347, 1998.

Mitasova, H. and Mitas, L.: Interpolation by regularized spline with tension: I. Theory and implementation, Mathematical Geology, 25, 641–655, https://doi.org/10.1007/BF00893171, 1993.

Mitasova, H. and Mitas, L.: Multiscale soil erosion simulations for land use management, in: Landscape erosion and evolution modeling, edited by Harmon, R. S. and Doe, W. W., chap. 11, pp. 321–347, Springer, Boston, MA, https://doi.org/10.1007/978-1-4615-0575-4_11, 2001.

Mitasova, H., Hofierka, J., Zlocha, M., and Iverson, L. R.: Modelling topographic potential for erosion and deposition using GIS, International Journal of Geographical Information Science, 10, 629–641, https://doi.org/10.1080/02693799608902101, http://dx.doi.org/10.1080/02693799608902101, 1996.

Mitasova, H., Thaxton, C., Hofierka, J., McLaughlin, R., Moore, A., and Mitas, L.: Path sampling method for modeling overland water flow, sediment transport, and short term terrain evolution in Open Source GIS, Developments in Water Science, 55, 1479–1490, https://doi.org/10.1016/S0167-5648(04)80159-X, 2004.

Mitasova, H., Mitas, L., and Harmon, R. S.: Simultaneous spline approximation and topographic analysis for lidar elevation data in open-source GIS, IEEE Geoscience and Remote Sensing Letters, 2, 375–379, https://doi.org/10.1109/LGRS.2005.848533, 2005.

Mitasova, H., Barton, M., Ullah, I., Hofierka, J., and Harmon, R.: 3.9 GIS-Based Soil Erosion Modeling, in: Treatise on Geomorphology, edited by Shroder, J. F., chap. 3.9, pp. 228–258, Elsevier, San Diego, California, USA, https://doi.org/10.1016/B978-0-12-374739-6.00052-X, http://www.sciencedirect.com/science/article/pii/B978012374739600052X, 2013.

Moore, I. and Burch, G.: Modeling Erosion and Deposition: Topographic Effects, Transactions of the American Society of Agricultural Engineers, 29, 1624–1640, 1986.

North Carolina Risk Management Office: QL2 / QL1 LiDAR Collection, Tech. rep., https://sdd.nc.gov/sdd/docs/LiDARSummary.pdf, 2018.

Panagos, P., Ballabio, C., Borrelli, P., Meusburger, K., Klik, A., Rousseva, S., Tadić, M. P., Michaelides, S., Hrabalíková, M., Olsen, P., Aalto, J., Lakatos, M., Rymszewicz, A., Dumitrescu, A., Beguería, S., and Alewell, C.: Rainfall erosivity in Europe, Science of the Total Environment, 511, 801–814, https://doi.org/10.1016/j.scitotenv.2015.01.008, 2015.

Panagos, P., Borrelli, P., Meusburger, K., Yu, B., Klik, A., Jae Lim, K., Yang, J. E., Ni, J., Miao, C., Chattopadhyay, N., Sadeghi, S. H., Hazbavi, Z., Zabihi, M., Larionov, G. A., Krasnov, S. F., Gorobets, A. V., Levi, Y., Erpul, G., Birkel, C., Hoyos, N., Naipal, V., Oliveira, P. T. S., Bonilla, C. A., Meddi, M., Nel, W., Al Dashti, H., Boni, M., Diodato, N., Van Oost, K., Nearing, M., and Ballabio, C.: Global rainfall erosivity assessment based on high-temporal resolution rainfall records, Scientific Reports, 7, 4175, https://doi.org/10.1038/s41598-017-04282-8, http://www.nature.com/articles/s41598-017-04282-8, 2017.

Perroy, R. L., Bookhagen, B., Asner, G. P., and Chadwick, O. A.: Comparison of gully erosion estimates using airborne and ground-based LiDAR on Santa Cruz Island, California, Geomorphology, 118, 288 – 300, https://doi.org/https://doi.org/10.1016/j.geomorph.2010.01.009, http://www.sciencedirect.com/science/article/pii/S0169555X10000358, 2010.

Renard, K. G., Foster, G. R., Weesies, G. A., McCool, D. K., and Yoder, D. C.: Predicting soil erosion by water: a guide to conservation planning with the Revised Universal Soil Loss Equation (RUSLE), Tech. Rep. 703, US Government Printing Office, Washington, DC, https://www.ars.usda.gov/ARSUserFiles/64080530/rusle/ah_703.pdf, 1997.

Roo, A., , A., Wesseling, C., Jetten, V., and Ritsema, C.: LISEM: A physically-based hydrological and soil erosion model incorporated in a GIS, In: K. Kovar & H.P. Nachtnebel (eds.), Application of geographic information systems in hydrology and water resources management. Wallingford (UK), IAHS, 1996. IAHS Publ. 235, pp. 395-403, 1996.

Schoorl, J., Veldkamp, A., and Bouma, J.: Modeling Water and Soil Redistribution in a Dynamic Landscape Context, Soil Science Society of American Journal, 66, 1610–1619, 2002.

Schoorl, J. M., Sonneveld, M. P. W., and Veldkamp, A.: Three-dimensional landscape process modelling: the effect of DEM resolution, Earth Surface Processes and Landforms, 25, 1025–1034, https://doi.org/10.1002/1096-9837(200008)25:9<1025::AID-ESP116>3.0.CO;2-Z, https://onlinelibrary.wiley.com/doi/abs/10.1002/1096-9837%28200008%2925%3A9%3C1025%3A%3AAID-ESP116%3E3.0.CO%3B2-Z, 2000.

Shobe, C. M., Tucker, G. E., and Barnhart, K. R.: The SPACE 1.0 model: A Landlab component for 2-D calculation of sediment transport, bedrock erosion, and landscape evolution, Geoscientific Model Development, 10, 4577–4604, https://doi.org/10.5194/gmd-10-4577-2017, 2017.

Sorrie, B. A.: An Inventory of the Significant Natural Areas of Hoke County, North Carolina, Tech. rep., North Carolina Natural Heritage Program, 2004.

Sorrie, B. A., Gray, J. B., and Crutchfield, P. J.: The Vascular Flora of the Longleaf Pine Ecosystem of Fort Bragg and Weymouth Woods, North Carolina, Castanea, 71, 129–161, https://doi.org/10.2179/05-02.1, 2006.

Starek, M. J., Mitasova, H., Hardin, E., Weaver, K., Overton, M., and Harmon, R. S.: Modeling and analysis of landscape evolution using airborne , terrestrial , and laboratory laser scanning, Geosphere, 7, 1340–1356, https://doi.org/10.1130/GES00699.1, 2011.

Telling, J., Lyda, A., Hartzell, P., and Glennie, C.: Review of Earth science research using terrestrial laser scanning, Earth-Science Reviews, 169, 35 – 68, https://doi.org/https://doi.org/10.1016/j.earscirev.2017.04.007, http://www.sciencedirect.com/science/article/pii/S0012825216304433, 2017.

Temme, A., Schoorl, J., Claessens, L., and Veldkamp, A.: 2.13 Quantitative Modeling of Landscape Evolution, vol. 2, Elsevier Ltd., https://doi.org/10.1016/B978-0-12-374739-6.00039-7, http://linkinghub.elsevier.com/retrieve/pii/B9780123747396000397, 2013.

Thaxton, C. S.: Investigations of grain size dependent sediment transport phenomena on multiple scales, Phd, North Carolina State University, http://www.lib.ncsu.edu/resolver/1840.16/3339, 2004.

Thomas, J. T., Iverson, N. R., Burkart, M. R., and Kramer, L. A.: Long-term growth of a valley-bottom gully, Western Iowa, Earth Surface Processes and Landforms, 29, 995–1009, https://doi.org/10.1002/esp.1084, 2004.

Tucker, G., Lancaster, S., Gasparini, N., and Bras, R.: The channel-hillslope integrated landscape development model (CHILD), in: Landscape erosion and evolution modeling, pp. 349–388, Springer, Boston, MA, https://doi.org/10.1007/978-1-4615-0575-4_12, 2001.

Tucker, G. E. and Hancock, G. R.: Modelling landscape evolution, Earth Surface Processes and Landforms, 35, 28–50, https://doi.org/10.1002/esp.1952, https://onlinelibrary.wiley.com/doi/abs/10.1002/esp.1952, 2010.

Tucker, G. E. and Slingerland, R. L.: Erosional dynamics, flexural isostasy, and long-lived escarpments: A numerical modeling study, Journal of Geophysical Research: Solid Earth, 99, 12 229–12 243, https://doi.org/10.1029/94JB00320, https://agupubs.onlinelibrary.wiley.com/doi/abs/10.1029/94JB00320, 1994.

Webb, R. and Wilshire, H.: Environmental Effects of Off-Road Vehicles: Impacts and Management in Arid Regions, Environmental Management Series, Springer New York, https://doi.org/10.1007/978-1-4612-5454-6, 1983.

Willgoose, G.: Mathematical Modeling of Whole Landscape Evolution, Annual Review of Earth and Planetary Sciences, 33, 443–459, https://doi.org/10.1146/annurev.earth.33.092203.122610, http://www.annualreviews.org/doi/10.1146/annurev.earth.33.092203.122610, 2005.

Wischmeier, W. H., Smith, D. D., Science, U. S., Administration, E., and Station, P. U. A. E.: Predicting Rainfall Erosion Losses: A Guide to Conservation Planning, Tech. rep., Washington, D.C., https://naldc.nal.usda.gov/download/CAT79706928/, 1978.

Yang, S., Guan, Y., Zhao, C., Zhang, C., Bai, J., and Chen, K.: Determining the influence of catchment area on intensity of gully erosion using high-resolution aerial imagery: A 40-year case study from the Loess Plateau, northern China, Geoderma, 347, 90 – 102, https://doi.org/https://doi.org/10.1016/j.geoderma.2019.03.042, http://www.sciencedirect.com/science/article/pii/S0016706118312230, 2019.

Yin, S., A. Nearing, M., Borrelli, P., and Xue, X.: Rainfall Erosivity: An Overview of Methodologies and Applications, Vadose Zone Journal, 16, https://doi.org/10.2136/vzj2017.06.0131, 2017.

Zahra, T., Paudel, U., Hayakawa, Y., and Oguchi, T.: Knickzone Extraction Tool (KET) – A New ArcGIS toolset for automatic extraction of knickzones from a DEM based on multi-scale stream gradients, Open Geosciences, 9, https://doi.org/10.1515/geo-2017-0006, 2017.